

A Structural, Kinetic, and Thermodynamic Study of the Reversible Thermal C-H Activation/Reductive Elimination of Alkanes at Iridium

J. Michael Buchanan, Jeffrey M. Stryker, and Robert G. Bergman*

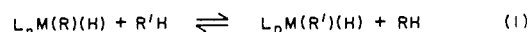
Contribution from the Department of Chemistry, University of California, and Materials and Molecular Research Division, Lawrence Berkeley Laboratory, Berkeley, California 94720.

Received July 16, 1985

Abstract: The hydrido alkyl iridium complex $\text{Cp}^*(\text{PMe}_3)\text{Ir}(\text{Cy})(\text{H})$ (**1**, $\text{Cp}^* = \eta^5\text{-C}_5\text{Me}_5$; $\text{Cy} = \text{cyclohexyl}$) has been isolated by air-free chromatography at -80°C , and its molecular structure has been determined by X-ray diffraction. Thermolysis of **1** in benzene cleanly produces cyclohexane and $\text{Cp}^*(\text{PMe}_3)\text{Ir}(\text{Ph})(\text{H})$ (**2**). The rate of the reaction is first-order in **1**, zero-order in benzene, and inhibited by cyclohexane; its activation parameters are $\Delta H^\ddagger = 35.6 \pm 0.5 \text{ kcal/mol}$ and $\Delta S^\ddagger = +10 \pm 2 \text{ eu}$. An inverse isotope effect, $k_h/k_d = 0.7 \pm 0.1$, is calculated from rates of cyclohexane and cyclohexane- d_{12} reductive elimination at 130°C , and deuterium scrambling between the hydride and α -cyclohexyl positions is observed to occur competitively with reductive elimination. A mechanism is proposed in which cyclohexane loss from **1** is reversible and produces $[\text{Cp}^*(\text{PMe}_3)\text{Ir}]$, which oxidatively adds to a C-H bond in a benzene solvent molecule to form **2**. Evidence is also presented for the possible intermediacy of a cyclohexane/ $[\text{Cp}^*(\text{PMe}_3)\text{Ir}]$ σ -complex, which is formed before free $[\text{Cp}^*(\text{PMe}_3)\text{Ir}]$ is released. Equilibrium constants for the equilibration of several pairs of alkanes and their corresponding iridium(III) hydrido alkyl complexes have been determined and imply the following trend in solution phase iridium-carbon bond dissociation enthalpies: phenyl $\gg n$ -pentyl $> 2,3$ -dimethylbutyl $>$ cyclopentyl \sim cyclohexyl $>$ neopentyl.

Interest in reactions of alkanes and arenes with metal complexes has led to the discovery of many examples of intermolecular carbon-hydrogen bond activation.¹⁻³ Some of these appear to be radical processes in which a hydrogen atom is abstracted from the hydrocarbon.² Others may involve electrophilic attack of metal complexes on C-H bonds.³ The majority of examples appear to involve what is formally⁴ an oxidative addition of a C-H bond to a coordinatively unsaturated metal center.¹ Surprisingly, very few complete mechanistic studies of C-H activation have been carried out. This is especially true of alkane activation, because, until recently, so few examples of this process were known. Ideally suited to study, then, are those reactions in which (a) both the organometallic reactant and product are simple hydrido alkyl or hydrido aryl metal complexes, (b) the overall transformation involves only oxidative addition and reductive elimination of the

hydrocarbons (eq 1), and (c) the reaction can be observed to occur in both the forward and reverse direction.



We report here the results of two studies on such a system, specifically that where $\text{L}_n\text{M} = \text{Cp}^*(\text{PMe}_3)\text{Ir}$.⁵ In the first study the two hydrocarbons are chosen so that the reaction proceeds only in the forward direction, facilitating mechanistic experiments. In the second study we demonstrate for the first time the reversibility of alkane reactions of the type shown in eq 1. In this instance pairs of hydrocarbon solvents are chosen to balance energetically the reaction, allowing determination of equilibrium constants from which the relative iridium-carbon bond dissociation enthalpies are estimated.

Results

Synthesis, Characterization, and X-ray Crystal Structure of $\text{Cp}^*(\text{PMe}_3)\text{Ir}(\text{Cy})(\text{H})$ (1**).** The starting material for these studies has been described and partially characterized previously as the product of cyclohexane C-H activation in the photolysis of $\text{Cp}^*(\text{PMe}_3)\text{Ir}(\text{H})_2$ in cyclohexane.^{1k} A preliminary report of its thermal chemistry has appeared.⁶ Although **1** is remarkably thermally robust for a hydrido alkyl complex, initial attempts at purification were foiled by its sensitivity to chromatography supports and its high solubility in hydrocarbon solvents. We have since been able to obtain sharp-melting, analytically pure **1** using air-free chromatography on alumina III at -80°C , or direct crystallization from very highly concentrated hexamethyldisiloxane or pentane solutions, as described in the Experimental Section. This complex has been characterized by ^1H NMR, ^{13}C NMR, ^{31}P NMR, IR, carbon and hydrogen elemental analyses, and X-ray diffraction (see below). All spectral data are consistent with a pseudooctahedral or "three-legged piano stool" geometry for **1**, in which the phosphine, hydride, and cyclohexyl ligands occupy three facially related coordination sites and the pentamethylcyclopentadienyl ligand occupies the other three sites.

Slow recrystallization from pentane at -40°C afforded very pale yellow columnar crystals of diffraction quality, and an X-ray structure determination was undertaken. Crystal structures of mononuclear hydrido alkyl transition-metal complexes are rare

(1) (a) Chatt, J.; Davidson, J. M. *J. Chem. Soc.* **1965**, 843-855. (b) Rausch, M. D.; Gastinger, R. G.; Gardner, S. A.; Brown, R. K.; Wood, J. S. *J. Am. Chem. Soc.* **1977**, *99*, 7870-7876. (c) Tolman, C. A.; Ittel, S. D.; English, A. D.; Jesson, J. P. *Ibid.* **1979**, *101*, 1742-1751. (d) Crabtree, R. H.; Mihelcic, J. M.; Quirk, J. M. *Ibid.* **1979**, *101*, 7738-7740. (e) Crabtree, R. H.; Demou, P. C.; Eden, D.; Mihelcic, J. M.; Parnell, C. A.; Quirk, J. M.; Morris, G. E. *Ibid.* **1982**, *104*, 6994-7001. (f) Cooper, N. J.; Green, M. L. H.; Mahtab, R. *J. Chem. Soc., Dalton Trans.* **1979**, 1557-1562. (g) Berry, M.; Elmitt, K.; Green, M. L. H. *Ibid.* **1979**, 1950-1958. (h) Baudry, D.; Ephritikhine, M.; Felkin, H. *J. Chem. Soc., Chem. Commun.* **1980**, 1243-1244. (i) Werner, R.; Werner, H. *Angew. Chem., Int. Ed. Engl.* **1981**, *20*, 793-794. (j) Gomez, M.; Robinson, D. J.; Maitlis, P. M. *J. Chem. Soc., Chem. Commun.* **1983**, 825-826. (k) Janowicz, A. H.; Bergman, R. G. *J. Am. Chem. Soc.* **1983**, *105*, 3929-3939. (l) Periana, R. A.; Bergman, R. G. *Organometallics* **1984**, *3*, 508-510. (m) Hoyano, J. K.; McMaster, A. D.; Graham, W. A. G. *J. Am. Chem. Soc.* **1983**, *105*, 7190-7191. (n) Jones, W. D.; Feher, F. J. *Ibid.* **1984**, *106*, 1650-1663. (o) Morris, R. H.; Shiralian, M. *J. Organomet. Chem.* **1984**, *260*, C47-C51.

(2) (a) Groves, J. T.; Nemo, T. E. *J. Am. Chem. Soc.* **1983**, *105*, 6243-6248. (b) Smegal, J. A.; Schardt, B. C.; Hill, C. L. *Ibid.* **1983**, *105*, 3515-3521. (c) Mimoun, H.; Saussine, L.; Daire, E.; Postel, M.; Fischer, J.; Weiss, R. *Ibid.* **1983**, *105*, 3101-3110. (d) Traylor, T. G. *J. Chem. Soc., Chem. Commun.* **1984**, 279-280. (e) Wayland, B. B.; Del Rossi, K. J. *J. Organomet. Chem.* **1984**, *276*, C27-C30.

(3) (a) Shilov, A. E. *Pure Appl. Chem.* **1978**, *50*, 725-733. (b) Shul'pin, G. B.; Nizova, G. V.; Shilov, A. E. *J. Chem. Soc., Chem. Commun.* **1983**, 671-672. (c) Watson, P. L. *Ibid.* **1983**, 267-277. (d) Watson, P. L. *J. Am. Chem. Soc.* **1983**, *105*, 6491-6493. (e) Fendrick, C. M.; Marks, T. J. *Ibid.* **1984**, *106*, 2214-2216. (f) Thompson, M. E.; Bercaw, J. E. *Pure Appl. Chem.* **1984**, *56*, 1-11.

(4) While the formal oxidation state of a metal increases by two units when new bonds are made to carbon and hydrogen (e.g., $\text{M}^0 + \text{R-H} \rightarrow \text{M}^{\text{II}}(\text{R})(\text{H})$), such processes need not involve significant charge transfer from the metal atom to the hydride and alkyl ligands: (a) Low, J. J.; Goddard, W. A. *J. Am. Chem. Soc.* **1984**, *106*, 8321. (b) Crabtree, R. H.; Hlatky, G. C. *Inorg. Chem.* **1980**, *19*, 572-574.

(5) Abbreviations: $\text{Cp}^* = \eta^5\text{-C}_5(\text{CH}_3)_5$, pentamethylcyclopentadienyl; $\text{Cy} = \text{c-C}_6\text{H}_{11}$, cyclohexyl; $\text{Ph} = \text{C}_6\text{H}_5$, phenyl; $\text{PMe}_3 = \text{P}(\text{CH}_3)_3$, trimethylphosphine; $\text{PPh}_3 = \text{triphenylphosphine}$.

(6) Wax, M. J.; Stryker, J. M.; Buchanan, J. M.; Kovac, C. A.; Bergman, R. G. *J. Am. Chem. Soc.* **1984**, *106*, 1121-1122.

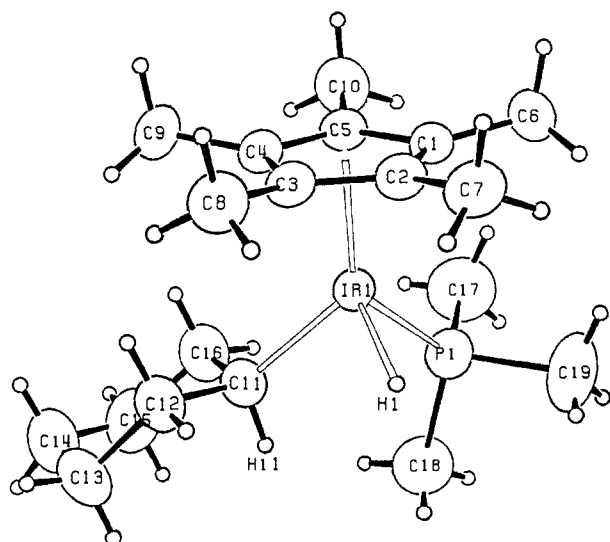


Figure 1. Molecular geometry and labeling scheme for molecule 1 of $\text{Cp}^*(\text{PMe}_3)\text{Ir}(\text{Cy})(\text{H})$ (**1**). The ellipsoids are scaled to represent the 50% probability surface. Hydrogen atoms are given as arbitrarily small spheres for clarity.

and appear to be limited to alkyl substituents lacking β -hydrogens or otherwise stabilized.⁷ The crystal structure consists of two independent molecules of $\text{Cp}^*(\text{PMe}_3)\text{Ir}(\text{Cy})(\text{H})$ in the asymmetric unit, related by pseudotranslational symmetry. Peaks corresponding to most of the hydrogen atoms, including the two iridium-bound hydrogens, were located directly in a difference Fourier map calculated following refinement of all non-hydrogen atoms with anisotropic thermal parameters. The positions of all hydrogen atoms were refined isotropically. The final residuals were $R = 2.17\%$ and $wR = 2.54\%$.

The two molecules in the unit cell are essentially identical. An ORTEP projection of one of these molecules and the labeling scheme are given in Figure 1. Interatomic bond distances and intramolecular bond angles for both molecules are presented in Tables I and II. Positional parameters for both molecules are included as supplementary material.

The structure reveals the expected pseudooctahedral geometry, although there are systematic distortions in all the ligands due to steric crowding in the molecule. The primary distortions are a movement of the methyl groups of the C_5Me_5 ligands out of plane away from the metal and other ligands, an increase of the angle Ir-P-C for the carbon closest to trans to the Cp^* (presumably due to the interaction with the α -carbon of the cyclohexyl group), and a slight increase relative to idealized tetrahedral geometry in the Ir-C-C angles around the α -carbon in the cyclohexyl group (presumably due to the interaction of the β -carbons with the Cp^* ring). Otherwise, both the cyclopentadiene and the cyclohexyl ligands are very regular. The ligand-metal-ligand bond angles for the phosphine, hydride, and cyclohexyl moieties deviate by less than 10° from the 90° angles anticipated for octahedral coordination. Several of the short intramolecular nonbonded contacts are noted in Table I. Inspection of a molecular model constructed from the crystallographic data indicated that these close contacts greatly constrain rotational motion in the molecule, doubtlessly contributing to our ability to locate and refine the hydride ligand positions. The crystallographically determined

(7) We are aware of no crystal structures of hydrido alkyl complexes having simple alkyl groups as ligands. However, several functionalized hydrido alkyl complexes have been structurally determined: (a) *cis*-(η^2 - C_5H_5)-(CO)₂Re(H)(CH₂Ph): Fischer, E. O.; Frank, A. *Chem. Ber.* **1978**, *111*, 3740. (b) *trans*-(Ph₃P)₂Pt(H)(CH₂CN): Pra, A. D.; Forsellini, E.; Bombieri, G.; Michelin, R. A.; Ros, R. *J. Chem. Soc., Dalton Trans.* **1979**, 1862. (c) (PMe₃)₃Ir(Cl)(H)(CH₂CHO): Milstein, D.; Calabrese, J. C. *J. Am. Chem. Soc.* **1982**, *104*, 3773. (d) (PMe₃)₄Ir(H)(CH₂OH)⁺PF₆⁻: Thorn, D. L.; Tulip, T. H. *Organometallics* **1982**, *1*, 1580. A variety of relevant mono- and dinuclear complexes in which the carbon substituent is part of an ortho metalated ligand and many compounds in which the α -carbon is sp² or sp hybridized have also been structurally characterized.⁸

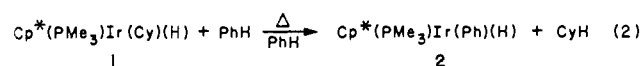
Table I. Selected Intramolecular Distances^a and Esd's (Å) for Complex 1

molecule 1			molecule 2		
atom 1	atom 2	distance	atom 1	atom 2	distance
Ir1	H1	1.55 (6)	Ir2	H2	1.62 (5)
Ir1	P1	2.215 (1)	Ir2	P2	2.216 (1)
Ir1	C1	2.269 (4)	Ir2	C21	2.302 (4)
Ir1	C2	2.237 (4)	Ir2	C22	2.264 (4)
Ir1	C3	2.239 (4)	Ir2	C23	2.248 (4)
Ir1	C4	2.302 (4)	Ir2	C24	2.239 (4)
Ir1	C5	2.301 (4)	Ir2	C25	2.299 (4)
Ir1	C11	2.125 (4)	Ir2	C31	2.141 (4)
Ir1	Cp1	1.915	Ir2	Cp2	1.920
C11	H11	1.02 (4)	C31	H31	1.09 (4)
C11	C12	1.516 (7)	C31	C32	1.524 (6)
C12	C13	1.552 (8)	C32	C33	1.536 (6)
C13	C14	1.514 (11)	C33	C34	1.532 (8)
C14	C15	1.497 (10)	C34	C35	1.500 (9)
C15	C16	1.533 (7)	C35	C36	1.537 (7)
C16	C11	1.513 (7)	C36	C31	1.522 (6)
P1	C17	1.816 (7)	P2	C37	1.811 (5)
P1	C18	1.811 (6)	P2	C38	1.827 (6)
P1	C19	1.822 (8)	P2	C39	1.813 (5)
C1	C2	1.423 (6)	C21	C22	1.432 (6)
C2	C3	1.435 (6)	C22	C23	1.409 (6)
C3	C4	1.433 (6)	C23	C24	1.435 (6)
C4	C5	1.417 (6)	C24	C25	1.433 (6)
C5	C1	1.449 (5)	C25	C21	1.427 (6)
C1	C6	1.491 (6)	C21	C26	1.497 (7)
C2	C7	1.491 (6)	C22	C27	1.511 (6)
C3	C8	1.504 (6)	C23	C28	1.505 (7)
C4	C9	1.497 (6)	C24	C29	1.498 (7)
C5	C10	1.482 (6)	C25	C30	1.500 (7)
Nonbonded Distances					
C17	C10	3.663 (10)	C39	C26	3.680 (9)
C19	C6	3.749 (11)	C38	C27	3.652 (9)
C18	C11	3.209 (8)	C37	C31	3.258 (8)
C9	C12	3.754 (8)	C30	C32	3.652 (7)
C9	C16	3.706 (8)	C30	C36	3.715 (8)
C8	C12	3.658 (8)	C29	C36	3.649 (7)

^a Cp1 and Cp2 are the centroids of the cyclopentadiene rings.

iridium-hydride bond lengths of 1.55 (6) and 1.62 (5) Å are consistent with each other and consistent with other terminal hydride ligand distances as determined by X-ray and neutron diffraction.⁸ The interatomic distance of 2.62 Å between the hydride ligand and cyclohexyl α -carbon precludes any bonding interaction; insertion into the cyclohexane C-H bond has clearly proceeded to completion. There are no abnormally short intermolecular distances in the crystals. No interaction between the hydrogen attached to C11 and the metal is observed.

Mechanistic Experiments. Thermolysis of $\text{Cp}^*(\text{PMe}_3)\text{Ir}(\text{Cy})(\text{H})$ in Benzene and Benzene- d_6 . When heated at 130°C , a 0.024 M solution of the cyclohexyl complex **1** in benzene decomposed cleanly and quantitatively to form free cyclohexane and $\text{Cp}^*(\text{PMe}_3)\text{Ir}(\text{Ph})(\text{H})$ (**2**) at a rate which was conveniently followed by ¹H NMR spectroscopy (eq 2). Cyclohexane was



identified on the basis of its characteristic chemical shift in benzene and by GC/MS (see below). Both the phenyl complex **2** and cyclohexane were quantified by ¹H NMR integration vs. internal hexamethyldisiloxane standard. The reaction is cleanly first order (data taken to >3 half-lives) in cyclohexyl complex **1** (eq 3) with

$$-\frac{d[\mathbf{1}]}{dt} = k_{\text{obs}}[\mathbf{1}] \quad (3)$$

$k_{\text{obs}} = 7.0 \times 10^{-5} \text{ s}^{-1}$ at 130°C . Measurement of the reaction

(8) (a) Tellet, R. G.; Bau, R. *Struct. Bonding* **1981**, *44*, 1 and references therein. (b) Moore, D. S.; Robinson, S. D. *Chem. Soc. Rev.* **1983**, *12*, 415 and references therein.

Table II. Interatomic Bond Angles^a and Esd's (deg) for 1

molecule 1				molecule 2			
atom 1	atom 2	atom 3	angle	atom 1	atom 2	atom 3	angle
Cp1	Ir1	P1	131.1	Cp2	Ir2	P2	131.0
Cp1	Ir1	C11	129.6	Cp2	Ir2	C31	129.2
Cp1	Ir1	H1	118.9	Cp2	Ir2	H2	122.6
P1	Ir1	C11	88.66 (13)	P2	Ir2	C31	89.24 (12)
P1	Ir1	H1	84.7 (21)	P2	Ir2	H2	81.5 (17)
C11	Ir1	H1	89.8 (20)	C31	Ir2	H2	87.9 (16)
Ir1	C11	H11	112.5 (23)	Ir2	C31	H31	101.5 (22)
Ir1	C11	C12	113.1 (3)	Ir2	C31	C32	113.4 (3)
Ir1	C11	C16	114.5 (3)	Ir2	C31	C36	113.1 (3)
C12	C11	C16	110.1 (4)	C32	C31	C36	109.8 (4)
Ir1	P1	C17	115.9 (3)	Ir2	P2	C37	120.25 (21)
Ir1	P1	C18	120.4 (3)	Ir2	P2	C38	114.44 (20)
Ir1	P1	C19	114.7 (3)	Ir2	P2	C39	116.59 (21)
C16	C11	H11	103.4 (23)	C32	C31	H31	107.5 (22)
C12	C11	H11	102.2 (23)	C36	C31	H31	111.2 (22)
C16	C11	C12	110.1 (4)	C36	C31	C32	109.8 (4)
C11	C12	C13	112.7 (5)	C31	C32	C33	112.4 (4)
C12	C13	C14	110.4 (6)	C32	C33	C34	111.0 (4)
C13	C14	C15	112.5 (6)	C33	C34	C35	111.3 (5)
C14	C15	C16	112.2 (5)	C34	C35	C36	111.6 (5)
C15	C16	C11	113.3 (6)	C35	C36	C31	112.6 (4)
C5	C1	C2	107.7 (3)	C25	C21	C22	106.8 (4)
C1	C2	C3	108.5 (3)	C21	C22	C23	109.2 (4)
C2	C3	C4	107.3 (3)	C22	C23	C24	108.1 (4)
C3	C4	C5	108.9 (3)	C23	C24	C25	107.1 (4)
C4	C5	C1	107.6 (3)	C24	C25	C21	108.7 (4)
C2	C1	C6	126.1 (4)	C22	C21	C26	128.0 (4)
C5	C1	C6	125.7 (4)	C25	C21	C26	124.7 (4)
C1	C2	C7	124.3 (4)	C21	C22	C27	124.6 (4)
C3	C2	C7	126.8 (4)	C23	C22	C27	125.6 (4)
C2	C3	C8	125.8 (4)	C22	C23	C28	125.3 (5)
C4	C3	C8	125.6 (4)	C24	C23	C28	126.3 (5)
C3	C4	C9	124.8 (4)	C23	C24	C29	127.2 (5)
C5	C4	C9	125.8 (4)	C25	C24	C29	124.6 (5)
C1	C5	C10	125.4 (4)	C21	C25	C30	125.5 (4)
C4	C5	C10	126.1 (4)	C24	C25	C30	125.3 (4)

^a Cp1 and Cp2 are the centroids of the cyclopentadiene rings.

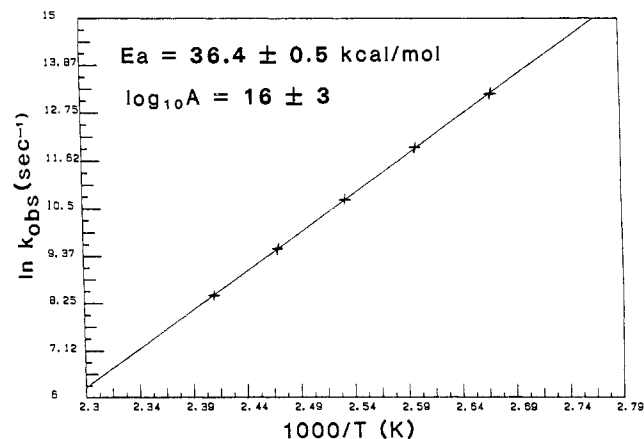


Figure 2. Arrhenius plot for thermolysis of cyclohexyl complex 1 in benzene over the temperature range 100–140 °C.

rate at five temperatures between 100 and 140 °C (Table III, experiment numbers 1–5) yielded the following activation parameters: $E_a = 36.4 \pm 0.5$ kcal/mol, $\log A = 16 \pm 3$, $\Delta H^\ddagger = 35.6 \pm 0.5$ kcal/mol, and $\Delta S^\ddagger = 10 \pm 2$ eu (Figure 2).

Decomposition of the cyclohexyl complex 1 in benzene- d_6 ⁹

(9) At extended reaction time, integration of hydride resonance of 1 vs. the Cp* and PMe₃ resonances suggested a small amount of deuterium incorporation into the hydride position, but the extent of this scrambling was insufficient to affect the kinetics. We suspect that the H/D scrambling is catalyzed by a coordinatively unsaturated trace impurity, as the addition of PMe₃ or PPh₃ to the reaction medium appears to prevent it. Alternatively, as suggested by a referee, this may be an intermolecular process involving interaction between starting material and product.

Table III. First-Order Rate Constants for the Disappearance of Cp*(PMe₃)Ir(C₆X₁₁)(X), X = H or D

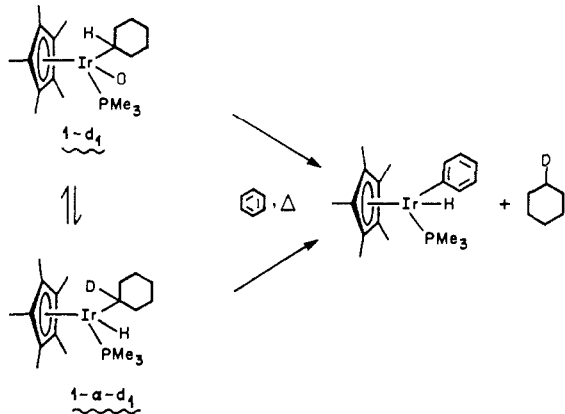
expt No.	X	solvent	temp (°C)	k_{obsd}^a (s ⁻¹)
1	H	C ₆ H ₆	100	1.8×10^{-6}
2	H	C ₆ H ₆	110	6.5×10^{-6}
3	H	C ₆ H ₆	120	2.2×10^{-5}
4	H	C ₆ H ₆	130	7.0×10^{-5}
5	H	C ₆ H ₆	140	2.1×10^{-4}
6	H	C ₆ D ₆ ^b	130	7.1×10^{-5}
7	D	C ₆ D ₆ ^b	130	1.0×10^{-4}
8	H	C ₆ H ₆ ^b	130	7.0×10^{-5}
9	H	C ₆ H ₆ ^b	130	7.0×10^{-5}
10	H	57 mol % C ₆ H ₆ /43 mol % neo-C ₅ H ₁₂ ^b	130	7.0×10^{-5}
11	H	16 mol % C ₆ H ₆ /84 mol % neo-C ₅ H ₁₂ ^b	130	7.0×10^{-5}
12	H	C ₆ H ₆ ^b	130	6.7×10^{-5}
13	H	83 mol % C ₆ H ₆ /17 mol % C ₆ H ₁₂ ^b	130	6.0×10^{-5}
14	H	71 mol % C ₆ H ₆ /29 mol % C ₆ H ₁₂ ^b	130	5.7×10^{-5}
15	H	54 mol % C ₆ H ₆ /46 mol % C ₆ H ₁₂ ^b	130	4.7×10^{-5}
16	H	26 mol % C ₆ H ₆ /74 mol % C ₆ H ₁₂ ^b	130	3.0×10^{-5}
17	H	16 mol % C ₆ H ₆ /84 mol % C ₆ H ₁₂ ^b	130	1.7×10^{-5}
18	H	8 mol % C ₆ H ₆ /92 mol % C ₆ H ₁₂ ^b	130	1.2×10^{-5}

^a All values $\pm 10\%$. ^b In the presence of PPh₃, ca. 0.05 M.

produced the phenyl complex 2- d_6 with no protons detected in the hydride or any of the aryl¹⁰ positions. Furthermore, the decomposition rate in benzene- d_6 (Table III, experiment no. 6) was indistinguishable from that in benzene.

(10) Jones and Feher¹⁰ found that the deuterium label in Cp*(PMe₃)Rh-(Ph)(D) was scrambled into the phenyl ring by a process involving η^2 -benzene complex intermediates.

Scheme I



Synthesis and Stability of $\text{Cp}^*(\text{PMe}_3)\text{Ir}(\text{Ph})(\text{H})$ (2**).** Independent synthesis of **2** was achieved in 39% yield by photolysis of $\text{Cp}^*(\text{PMe}_3)\text{Ir}(\text{H})_2$ in benzene,^{1k} followed by purification with room-temperature chromatography on alumina III. The complex has been characterized by ^1H NMR, ^{13}C NMR, ^{31}P NMR, IR, melting point, and carbon and hydrogen elemental analyses.

The stability of **2** to the reaction conditions was established by heating a benzene- d_6 solution of **2** in a sealed NMR tube and watching for a diminution in the intensity of bound aryl and hydride resonances relative to ferrocene internal standard. No exchange of bound benzene with bulk solvent was observed even after extended heating at 190 °C, 40 deg above the highest temperature at which kinetic measurements were made. This stands in contrast to the corresponding rhodium system, where arene exchange is observed at 60 °C.¹ⁿ

Synthesis and Thermolysis of $\text{Cp}^*(\text{PMe}_3)\text{Ir}(\text{Cy})(\text{D})$ (1-d₁**).** In an effort to measure a primary deuterium isotope effect for the loss of cyclohexane from the cyclohexyl complex **1**, we prepared the compound labeled specifically with deuterium in the hydride position. Treatment of $\text{Cp}^*(\text{PMe}_3)\text{Ir}(\text{Cy})(\text{Br})$ ^{1k} with sodium borodeuteride in isopropyl alcohol afforded a 95% yield of $\text{Cp}^*(\text{PMe}_3)\text{Ir}(\text{Cy})(\text{D})$ (**1-d₁**), whose extent of deuteration was estimated (NMR) at greater than 95%. The compound was identified on the basis of its ^1H NMR, ^2H NMR, ^{31}P NMR, and IR spectra. Thermolysis of a 0.02 M benzene solution of **1-d₁** at 130 °C revealed an unexpected result. In addition to the formation of free cyclohexane- d_1 and **2**, we observed a competitive process which exchanged deuterium between the hydride position and the α -position of the cyclohexyl ring (Scheme I), producing some **1- α -d₁**. The position of the deuterium in **1- α -d₁** was determined by comparison of its ^2H NMR chemical shift to the characteristic ^1H NMR chemical shift of the α -cyclohexyl proton of **1**.¹¹ No significant deuterium incorporation was observed in any other position of **1** at any point in the reaction, which was followed by greater than 90% conversion of **1-d₁** and **1- α -d₁** to phenyl complex **2**.

Furthermore, the rate constant for combined disappearance of **1-d₁** and **1- α -d₁** appeared to decrease as the reaction progressed, suggesting an inverse isotope effect for the loss of cyclohexane from **1**.

Thermolysis of **1-d₁** in cyclohexane at 130 °C was followed by ^2H NMR; this indicated that the rates of cyclohexane- d_1 loss and hydride to α -cyclohexyl H/D exchange are qualitatively comparable to rates for those processes in benzene.

A similar scrambling process has been observed in the hydrido methyl system. Deuterium scrambling between the hydride and the iridium-bound methyl group was observed (^1H NMR) when $\text{Cp}^*(\text{PMe}_3)\text{Ir}(\text{CH}_3)(\text{D})$ was heated at 125 °C in benzene- d_6 . In contrast to that observed in the hydrido cyclohexyl system, the scrambling is much faster than reductive elimination. Reductive elimination is also accompanied by slow decomposition to Cp^* -

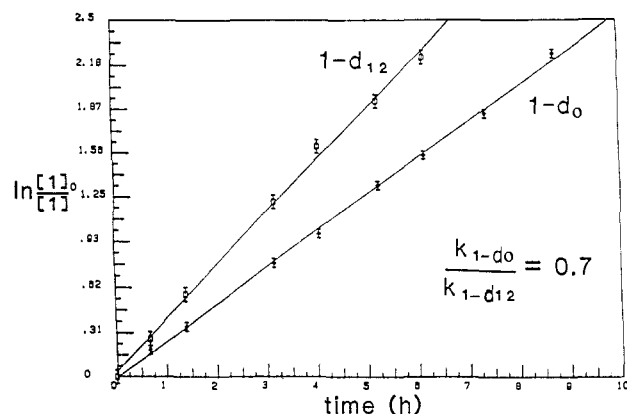


Figure 3. First-order kinetic plots for side-by-side thermolyses of cyclohexyl complexes **1-d₀** and **1-d₁₂** at 130 °C in benzene- d_6 with 0.05 M PPh_3 .

(PMe_3) IrD_2 , the formation of which is inhibited by added trimethylphosphine. In contrast to the hydrido cyclohexyl system, the reductive elimination is *not* cleanly unimolecular; 160 °C thermolysis of a benzene- d_6 solution of $\text{Cp}^*(\text{PMe}_3)\text{Ir}(\text{CH}_3)(\text{H})$ and $\text{Cp}^*(\text{PMe}_3)\text{Ir}(\text{CD}_3)(\text{D})$ produced a mixture of all possible methanes, $\text{CH}_n\text{D}_{4-n}$ ($n = 0-4$), after 65% combined conversion of starting materials. It is not clear whether the scrambling is the result of intermolecular interaction between the less sterically encumbered methyl complexes or due to catalysis by trace impurities or decomposition products. Because of these complications, details of the preparation of the labeled methyl complexes are given in the Experimental Section, but scrambling studies were confined to the more tractable cyclohexyl system.

Synthesis and Thermolysis of $\text{Cp}^*(\text{PMe}_3)\text{Ir}(\text{Cy}-d_{11})(\text{D})$ (1-d₁₂**).** Photolysis of $\text{Cp}^*(\text{PMe}_3)\text{Ir}(\text{H})_2$ ^{1k} in cyclohexane- d_{12} followed by heating the same reaction mixture at 150 °C for 55 min produced $\text{Cp}^*(\text{PMe}_3)\text{Ir}(\text{Cy}-d_{11})(\text{D})$ (**1-d₁₂**) in 41% yield after cold chromatography. This complex was characterized by ^1H NMR, ^2H NMR, ^{31}P NMR, and IR.

The kinetic isotope effect for cyclohexane loss was determined by heating **1** and **1-d₁₂** under strictly comparable conditions. Side-by-side thermolyses at 130 °C of 0.027 M solutions of **1** and **1-d₁₂** in benzene- d_6 with 0.053 M PPh_3 ⁹ were followed by ^1H NMR. Comparison of the observed rate constants (Table III, experiment numbers 7 and 8; Figure 3) revealed an *inverse* isotope effect, $k_1/k_{1-d_{12}} = 0.7 \pm 0.1$.

Thermolysis of **1 in the Presence of Added Phosphine.** When cyclohexyl complex **1** was heated at 100 °C in benzene- d_6 in the presence of PMe_3 (0.17 M) or PPh_3 (0.10 M) the reaction rate remained first order in **1**, and the observed rate constants were within 10% of that measured in the absence of added phosphine. As previously noted,⁹ added dative ligand prevents any observable hydrogen-deuterium exchange between the solvent and the hydride position of **1**.

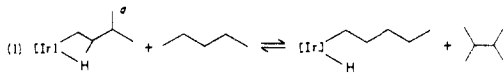
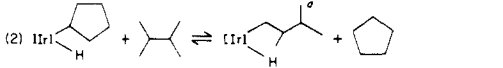
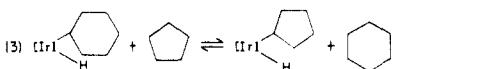
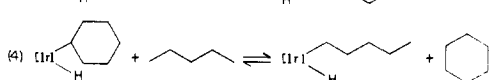
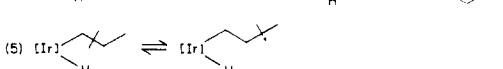
Thermolysis of a Mixture of **1 and **1-d₁₂** in Benzene.** To examine the molecularity of cyclohexane elimination, a benzene solution of cyclohexyl complexes **1** (0.020 M) and **1-d₁₂** (0.020 M) and PPh_3 (0.025 M) was heated at 130 °C. At intervals corresponding roughly to one-half, one, two, and four reaction half-lives, portions of the reaction mixture were removed and separated into volatile and nonvolatile components. GC/MS analysis of the volatile materials demonstrated that greater than 90%¹² of the cyclohexane was d_0 or d_{12} , indicating highly intramolecular mechanisms for cyclohexane elimination and H/D scrambling.

Dependence of Reaction Rate on Benzene Concentration. Determination of the reaction rate order at varying concentrations of benzene required the use of an inert diluent which would not alter the reaction stoichiometry or the solubility properties of the medium. Attempts to find a solvent which would not react with

(11) The α -hydrogen in unlabeled **1** was identified by ^1H - ^{13}C correlated two-dimensional NMR spectroscopy.

(12) This figure is based on a conservatively estimated 10% limit of delection. No direct evidence for cyclohexane- d_1 or $-d_{11}$ was observed.

Table IV. Equilibrium Constants for Alkane Exchange Reactions ($[\text{Ir}] = [\text{Cp}^*(\text{PMe}_3)\text{Ir}]$)

equilibrium	K_{eq} (140 °C)	ΔG° (140 °C), kcal/mol
(1) 	3.5	-1.0
(2) 	1.5	-0.3
(3) 	2.0	-0.6
(4) 	10.8 (10.5) ^b	-2.0 (-1.9) ^b
(5) 	≥20	≤-2.5

^a Two diastereomers of coincidentally equivalent energies. ^b Values in parentheses calculated from data for first three equilibria.

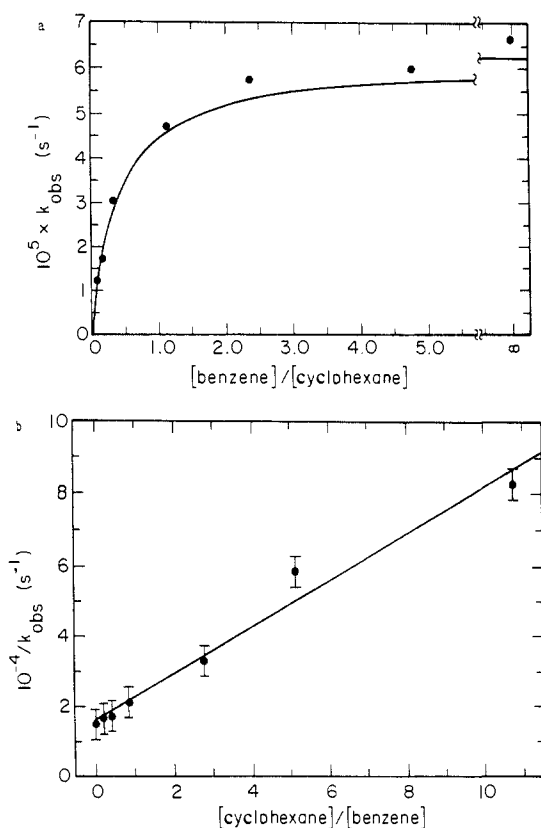


Figure 4. (a) Saturation plot showing the effect of added cyclohexane on k_{obs} . The solid line is calculated from best fit parameters derived from the linear plot, Figure 4b; (b) plot of $1/k_{\text{obs}}$ vs. $[\text{cyclohexane}]/[\text{benzene}]$, which is predicted to be linear by the rate law for mechanism a. Error bars represent one standard deviation.

the iridium species in solution and whose solutions with benzene could be liquefied under less than 20 atm of pressure at 130 °C were unsuccessful. The iridium intermediate reacted not only with all hydrocarbons tested but also with fluorocarbons (e.g., hexafluorobenzene) as well. We then sought an alkane whose corresponding C-H activation product would be unstable enough relative to the cyclohexyl complex **1** that its formation would be rapidly reversible and its concentration would not build up under the reaction conditions. Neopentane (2,2-dimethylpropane) met these criteria.

Three samples of cyclohexyl complex **1** (0.05 M) and PPh_3 (0.05 M) in benzene/neopentane mixtures corresponding to benzene

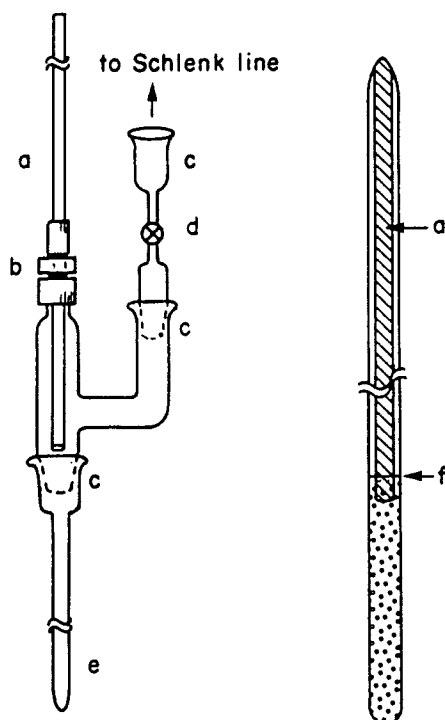


Figure 5. Apparatus for preparing low gas phase volume NMR sample tubes (left) and finished sample tube (right): (a) 3-mm Pyrex glass rod; (b) Cajon Ultratorr $3/8$ in. to $1/8$ in. adapter; (c) standard taper 14/20 joints; (d) 4-mm Kontes high-vacuum Teflon stopcock; (e) Wilmad 504PP medium-wall 5-mm NMR tube; (f) approximate solution level in sealed tube.

mole fractions of 1.0, 0.57, and 0.16 were heated at 130 °C, and the reactions were followed by ^1H NMR. Special sample tubes (see Figure 5 and Experimental Section) were used to ensure that the solvent composition remained virtually temperature independent between room temperature and 130 °C. First-order rate constants for all three samples were identical within experimental error (Table III, experiment numbers 9–11).

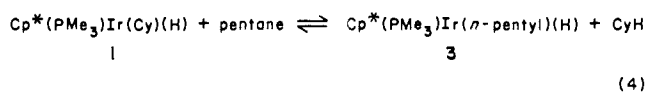
Dependence of Reaction Rate on Cyclohexane Concentration. We next investigated the effect of varying cyclohexane concentration on the rate of reductive elimination. Having demonstrated that the reaction rate was not dependent on benzene concentration, the neopentane diluent was no longer needed in these experiments. Seven samples of cyclohexyl complex **1** (0.05 M) and PPh_3 (0.06 M) in cyclohexane–benzene mixtures corresponding to molar concentration ratios of 0 (neat benzene), 0.21, 0.42, 0.86, 2.82, 5.20, and 10.84 were heated at 130 °C. The reactions were followed by ^1H NMR, and an amplitude modulated decoupling pulse was used to presaturate the solvent resonances. A significant inhibitory effect of cyclohexane was observed (Table III, exper-

iment numbers 12–18; Figure 4).

Thermodynamic Experiments. The equilibrium method and the derivation of thermodynamic data for the cyclohexane–pentane system will be described in detail. Results for other solvent pairs were obtained similarly and are summarized in tabular form (Table IV).

Synthesis and Characterization of $\text{Cp}^*(\text{PMe}_3)\text{Ir}(n\text{-pentyl})(\text{H})$ (3). This compound was reported previously as one of the products in the photolysis of $\text{Cp}^*(\text{PMe}_3)\text{Ir}(\text{H})_2$ in *n*-pentane and characterized after conversion to $\text{Cp}^*(\text{PMe}_3)\text{Ir}(n\text{-pentyl})(\text{Br})$.^{1k} We have now found that analytically pure 3 can be obtained in 41% yield from photolysis of the dihydride in *n*-pentane followed by thermolysis of the crude products for 21 h at 110 °C in *n*-pentane (to effect isomerization of secondary pentyl products to the *n*-pentyl product 3)^{1k} and air-free chromatography on alumina III at –80 °C. The complex, which is an oil at room temperature, has been characterized by ¹H NMR, ¹³C NMR, ³¹P NMR, IR, and carbon and hydrogen analyses.

Equilibration of $\text{Cp}^*(\text{PMe}_3)\text{Ir}(\text{Cy})(\text{H})$ and $\text{Cp}^*(\text{PMe}_3)\text{Ir}(n\text{-pentyl})(\text{H})$ in Cyclohexane/*n*-Pentane Mixtures. The equilibrium constant for the reaction illustrated in eq 4 was measured by heating either the *n*-pentyl complex 3 or the cyclohexyl complex 1 in a solvent mixture containing 91.5 mol % cyclohexane and



8.5 mol % *n*-pentane. After 50 h at 140 °C an equilibrium was reached in which the ratio of 3 to 1 was 1.0 ± 0.1 , as determined by ³¹P NMR.¹⁴ This allows calculation of an equilibrium constant of 10.8, which corresponds to $\Delta G^\circ = -2.0 \pm 0.2$ kcal/mol at 140 °C.

Two questions about the validity of the method come to mind: (a) is the system reaching a true equilibrium and (b) are we accurately evaluating the equilibrium ratios of alkanes and hydridoalkyliridium complexes? We believe the answer to both questions is yes. Our measured equilibrium constant is the same starting from either 1 or 3, and the same value is obtained in different cyclohexane/*n*-pentane mixtures. With respect to the second question we note the precautions taken to evaluate ratios of hydrocarbons and hydridoalkyliridium complexes. Solvent mixtures were prepared in approximately 100-mL batches by weighing each component of the mixture and calculating the molar ratio of alkanes from the ratio of masses. Also, each alkane was present in at least a 100-fold excess compared to the iridium species, and thermolyses were carried out in special NMR tubes (see Figure 5 and Experimental Section) to ensure that the solvent composition at equilibrium was the same (to within 1 or 2%) as the composition at the time of preparation. The ratio of hydridoalkyl complexes at equilibrium was determined by ³¹P NMR at room temperature, using parameters optimized for accurate integration. The combination of a slow approach to equilibrium at 140 °C and quick cooling of samples after heating ensured that the ratio of hydridoalkyliridium complexes was the same under equilibrium conditions as it was when we evaluated it. Overall, we estimate that the uncertainty in evaluating the equilibrium values is ± 5 –10%, the largest component being the uncertainty associated with the ³¹P NMR integrations.

Estimation of Relative Iridium–Carbon Bond Dissociation Enthalpies. Derivation of relative iridium–carbon bond dissociation enthalpies (BDEs), which are relative enthalpy values, from equilibrium constants requires separation of enthalpic and entropic components of $\Delta G^\circ_{\text{rxn}}$. Because the energy differences here are small, the temperature dependence of K_{eq} is very slight, and a plot of $\ln K_{\text{eq}}$ vs. T^{-1} is not sufficiently precise to permit accurate determinations of ΔH° and ΔS° . Instead, we think it is reasonable to make the assumption that $T\Delta S^\circ$ is close to zero.¹⁵

(14) Slow decomposition of 1 and 3 to $\text{Cp}^*(\text{PMe}_3)\text{Ir}(\text{H})_2$ takes place under these conditions, but the decomposition is slow enough that the equilibrium ratio of 1 and 3 is not perturbed.

Scheme II

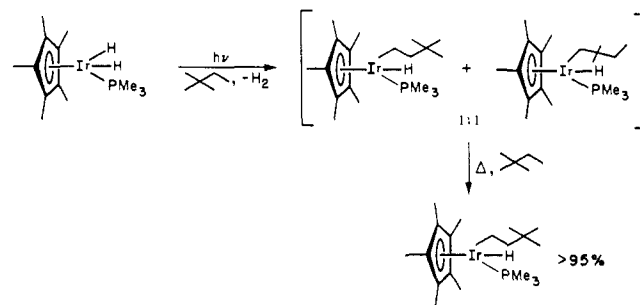


Table V. Relative Iridium–Carbon BDEs for Several Hydrido Alkyl Complexes ($[\text{Ir}] = [\text{Cp}^*(\text{PMe}_3)\text{Ir}]$)

compound	$\Delta D_{\text{Ir-C}}^a$	compound	$\Delta D_{\text{Ir-C}}^a$
	–4		4
	0		6
	0		$\geq 25^c$

^a All values ± 2 kcal/mol. ^b Two diastereomers of coincidentally equivalent energy. ^c A lower limit estimated on the basis of the kinetic stability of the complex (see text and ref 18).

From this we estimate that $\Delta H^\circ_{\text{rxn}} \approx -2.0$ kcal/mol in solution. Estimation of BDEs for the solution phase¹⁶ requires only the further assumption that solution-phase BDEs for the alkane carbon–hydrogen bonds do not differ significantly from tabulated gas-phase values.

Employing values of 95.5 and 98 kcal/mol respectively for the secondary C–H bond energy in cyclohexane and the primary C–H bond energy in *n*-pentane,¹⁷ we calculate that the iridium–*n*-pentyl bond is 5 ± 2 kcal/mol stronger than the iridium–cyclohexyl bond. Equilibrium constants for this and other alkane-exchange equilibria are presented in Table IV. Note that the fourth equilibrium is the sum of the first three. The product of the first three equilibrium constants is approximately equal to the experimentally measured fourth equilibrium constant; this serves as a check on the validity of the data.

The last equilibrium tabulated represents the *thermodynamic* preference for two types of C–H bonds in the *same* molecule, 2,2-dimethylbutane (Scheme II). The limit for the equilibrium constant was determined by heating a 1:1 mixture of the two isomers (obtained as a purified mixture following photolysis of $\text{Cp}^*(\text{PMe}_3)\text{Ir}(\text{H})_2$ in 2,2-dimethylbutane) at 140 °C for 20 h in 2,2-dimethylbutane and reflects our limit of detection.

Calculated relative iridium–carbon BDEs are presented in Table V. Given the uncertainties associated with the $\Delta D_{\text{M-C}}$ values, we believe the values are best interpreted as indicating the following qualitative trend in iridium–alkyl bond strengths: neopentyl < cyclohexyl \sim cyclopentyl < primary 2,3-dimethylbutyl < primary pentyl. The lower limit for the relative strength of the iridium–phenyl bond is a rough estimate based on the kinetic stability of the phenyl complex 2 in benzene-*d*₆.¹⁸ This calculation

(15) Because of the similarity of forward and reverse reactions, the translational component of ΔS° is almost certainly close to zero. Estimation of rotational and vibrational components is more complicated, but we believe that the contributions of $T\Delta S^\circ_{\text{rot}}$ and $T\Delta S^\circ_{\text{vib}}$ to ΔG° are likely to be no greater than our uncertainty in ΔG° .

(16) Other authors have also chosen to express metal carbon bond enthalpies as solution phase values. Cf.: (a) Halpern, *J. Acc. Chem. Res.* **1982**, *15*, 238–244. (b) Halpern, J.; Kim, S.-H.; Leung, T. W. *J. Am. Chem. Soc.* **1984**, *106*, 8317–8319.

(17) McMillen, D. F.; Golden, D. M. *Annu. Rev. Phys. Chem.* **1982**, *33*, 493–532.

implies that the iridium–phenyl bond is well over 25 kcal/mol stronger than the iridium–cyclohexyl bond. Again, one can compare this to the difference of 13 kcal/mol between $D_{\text{Rh-Ph}}$ and $D_{\text{Rh-Me}}$ calculated by Jones and Feher.¹¹

Discussion

Mechanistic Experiments. This work centers on the thermolysis of a hydridocyclohexyliridium(III) complex in benzene, which produces a stable hydridophenyliridium(III) complex (eq 2). In this reaction both C–H activation and reductive elimination of hydrocarbon occur at the same metal center.^{1f,n} While few thorough mechanistic investigations of C–H activation have been carried out, the reverse process, metal-mediated carbon–hydrogen bond formation, has been extensively studied,¹⁹ especially alkane reductive eliminations from hydridoalkylmetal complexes.²⁰ In these studies, four modes of alkane loss from *cis*-hydridoalkylmetal complexes have been postulated. These are adapted for the system under consideration and illustrated respectively in Schemes IIIa–d: (a) simple intramolecular reductive elimination;^{1f,n,20a} (b) reductive elimination preceded by a phosphine dissociation preequilibrium^{20e} and addition of benzene to give an Ir(V) intermediate; (c) reductive elimination preceded by reversible transfer of a hydrogen to a pentamethylcyclopentadienyl ligand;^{20f} and (d) intermolecular (binuclear) reductive elimination.^{20g,21} In addition to the precedented mechanisms, we considered three other types of mechanisms plausible: (e) (see Scheme IIIe) an $\eta^5\text{-Cp}^*$ to $\eta^3\text{-Cp}^*$ or “ring slip” preequilibrium,²² followed by benzene oxidative addition to form an iridium(V) intermediate which eliminates cyclohexane and restores the pentahapticity of Cp* ligand to give phenyl complex **2**; (f) any of several mechanisms which begin with iridium–cyclohexyl bond homolysis and include hydrogen atom abstraction by a free radical (note that these mechanisms would predict the same products in a crossover experiment as mechanism d); and (g) catalysis of the **1** to **2** conversion by an impurity.

Preliminary kinetic experiments revealed that heating the hydrido cyclohexyl complex **1** in benzene produced cyclohexane and hydrido phenyl complex **2** cleanly and quantitatively and that the reaction is first order in **1**. This observation alone is *not* sufficient to rule out a dinuclear reductive elimination, mechanism d. Norton and Okrasinski^{20g} observed first-order kinetics in dinuclear methane elimination from $\text{Os}(\text{CO})_4(\text{CH}_3)(\text{H})$, and such behavior is ex-

pected for any dinuclear elimination in which the rate-determining step is first order in the organometallic complex and precedes the association of two metal centers. The activation parameters $\Delta H^\ddagger = 35.6 \pm 0.5$ kcal/mol and $\Delta S^\ddagger = 10 \pm 2$ eu, while insufficient to conclusively rule out any of the proposed mechanisms, suggest that the rate-determining step is not associative (e.g., reaction of a benzene solvent molecule with an unsaturated iridium intermediate, as in mechanisms b, c, and e). The activation enthalpy is among the highest measured for reductive elimination from a hydrido alkyl complex²³ and attests to the remarkable thermal stability of the hydrido cyclohexyl complex **1**.

Thermolysis of **1** in benzene-*d*₆ produced phenyl complex **2-d**₆, with no detectable proton incorporation in either the hydride or aryl positions. This result is inconsistent with mechanism c, which predicts that the product would have a proton in the hydride position, i.e., the hydride in the product would be the same atom as the hydride in the starting material. We therefore discount mechanism c. Note also that for this result to be consistent with mechanisms b and e, the intermediates in those mechanisms with both hydrocarbons simultaneously bound must retain a stereochemistry in which the cyclohexyl ligand can only eliminate with the original hydride in **1** and *not* with the hydride derived from benzene addition. That the observed rate constant is identical in benzene and benzene-*d*₆ strongly suggests that the benzene C–H (C–D) bond is not being broken in the rate-determining step—a further constraint on mechanisms b and e.

The phosphine dissociation mechanism b can be ruled out by the failure of added PMe_3 to significantly perturb the reaction rate. The lack of phosphine inhibition also rules out mechanisms in which phosphine dissociation is followed by cyclohexane reductive elimination to form the 14-electron fragment, Cp^*Ir , which would then be trapped, in either order, by benzene and phosphine to form the hydrido phenyl complex **2**. The lack of phosphine inhibition, taken with the high reproducibility of rate constants from batch to batch of cyclohexyl complex **1**, suggests that the **1** to **2** conversion is not being catalyzed by a trace impurity (mechanism g).

Mechanism d, dinuclear reductive elimination, and mechanism f, iridium–cyclohexyl bond homolysis, were tested with a crossover experiment. When a mixture of **1** and **1-d**₁₂ was heated in benzene, the cyclohexane formed was >90% *d*₀ and *d*₁₂, implying that cyclohexane formation is a highly intramolecular process. Hence mechanisms d and f may be ruled out as major reaction pathways.

The remaining mechanisms, a and e, can be distinguished by considering the dependence of k_{obsd} on cyclohexane concentration. Thermolysis of **1** in cyclohexane–benzene mixtures (Table III) revealed that the reaction rate is inhibited by cyclohexane. We believe this is the first instance in which alkane reductive elimination from $\text{L}_n\text{M}(\text{R})(\text{H})$ has been inhibited by added alkane. Reconciliation of this result with the ring-slip mechanism e requires that step –13 is competitive with step 14. Thus, oxidative addition of cyclohexane to $(\eta^3\text{-Cp}^*)(\text{PMe}_3)\text{Ir}(\text{Ph})(\text{H})$ must be competitive with resymmetrization of the Cp* ring in that intermediate, even at the lowest studied concentration (ca. 2 M in each case) of added cyclohexane. We consider this very unlikely. Note that cyclohexane inhibition is expected for mechanism a as long as the kinetic selectivity of $\text{Cp}^*(\text{PMe}_3)\text{Ir}$ for benzene over cyclohexane (i.e., k_2/k_{-1}) is not very large. As shown in Figure 4b, a plot of $1/k_{\text{obsd}}$ vs. $[\text{cyclohexane}]/[\text{benzene}]$ is linear, so cyclohexane inhibition is consonant with the rate expression for mechanism a (eq 5).

$$\frac{1}{k_{\text{obsd}}} = \frac{k_{-1}[\text{C}_6\text{H}_{12}]}{k_1 k_2 [\text{PhH}]} + \frac{1}{k_1} \quad (5)$$

(23) McCarthy, T. J.; Nuzzo, R. G.; Whitesides, G. M. *J. Am. Chem. Soc.* **1981**, *103*, 3396–3403. Whitesides and co-workers have determined activation parameters, $\Delta H^\ddagger = 45 \pm 3$ kcal/mol and $\Delta S^\ddagger = 35 \pm 5$ eu, for the thermolysis of $(\text{Et}_3\text{P})_2\text{Pt}(\text{CH}_2\text{CH}_3)_2$ in the presence of 0.3 M PEt_3 , which produces $(\text{Et}_3\text{P})\text{Pt}(\text{C}_2\text{H}_5)$, ethane, and PEt_3 . Although the rate-determining step is postulated to be ethane reductive elimination from the intermediate $(\text{Et}_3\text{P})(\text{C}_2\text{H}_5)\text{Pt}(\text{CH}_2\text{CH}_3)(\text{H})$, the activation parameters are probably best considered an energetic composite of the reductive elimination and the phosphine dissociation and β -elimination which precede it.

(18) With use of a lower limit of 50 h for the half-life of **2** in benzene-*d*₆ at 200 °C, the minimum rate constant for benzene reductive elimination is $k_{\text{IrPh}}(200^\circ\text{C}) \leq 4 \times 10^{-6} \text{ s}^{-1}$ (hence, $\Delta G^\ddagger_{\text{IrPhH}}(200^\circ\text{C}) \geq 35$ kcal/mol). The activation parameters for cyclohexane reductive elimination permit calculation of the rate constant for cyclohexane elimination from **1** in benzene at 200 °C: $k_{\text{IrC}_6\text{H}_{12}}(200^\circ\text{C}) = 6 \times 10^{-2} \text{ s}^{-1}$ ($\Delta G^\ddagger_{\text{IrC}_6\text{H}_{12}}(200^\circ\text{C}) \approx 27$ kcal/mol). With these figures and an estimate of ΔG^\ddagger based on the kinetic preference of the intermediate for benzene over cyclohexane, we can calculate $\Delta G^\circ(200^\circ\text{C}) = \Delta G^\ddagger_{\text{IrC}_6\text{H}_{12}}(200^\circ\text{C}) - \Delta G^\ddagger_{\text{IrPhH}}(200^\circ\text{C}) - \Delta G^\ddagger(200^\circ\text{C}) \leq 27 - 35 - 1 = -9$ kcal/mol. If we assume, as before, that $\Delta H^\circ \approx \Delta G^\circ$, then $D_{\text{Ir-Ph}} - D_{\text{Ir-C}_6\text{H}_{12}} \geq 9 + 111 - 95 = 25$ kcal/mol.

(19) For a recent review, see: Halpern, J. *Acc. Chem. Res.* **1982**, *15*, 332–338.

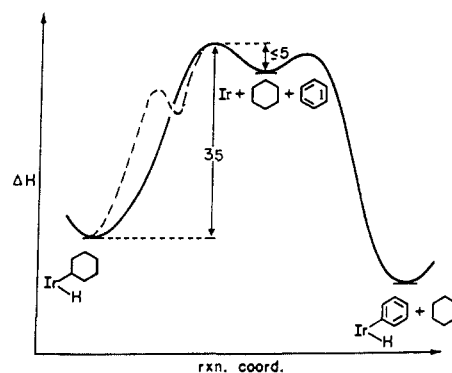
(20) See ref 1f,n and the following: (a) Abis, L.; Sen, A.; Halpern, J. *J. Am. Chem. Soc.* **1978**, *100*, 2915–2916. (b) Michelin, R. A. *Inorg. Chem.* **1983**, *22*, 1831–1834. (c) Halpern, J. *Acc. Chem. Res.* **1982**, *15*, 332–338. (d) Bullock, R. M.; Headford, C. E. L.; Kegley, S. E.; Norton, J. R. *J. Am. Chem. Soc.* **1985**, *107*, 727–729. (e) Milstein, D. *Acc. Chem. Res.* **1984**, *17*, 221–226. (f) McAlister, R. R.; Erwin, D. K.; Bercau, J. E. *J. Am. Chem. Soc.* **1978**, *100*, 5966–5968. (g) Norton, J. *Acc. Chem. Res.* **1979**, *12*, 139–145. References 1n and 20d describe reductive elimination from $\text{Cp}_2\text{W}(\text{Me})(\text{H})$; the elimination itself is intramolecular but at high concentrations is preceded by a dinuclear process which scrambles hydrogen (deuterium) atoms between the hydride position of one molecule and the methyl position of the other.

(21) To our knowledge, ref 20g describes the only established example of binuclear reductive elimination of R–H from a mononuclear *cis*-hydrido alkyl complex. This type of elimination is much more common in reactions of metal alkyls with metal hydrides. See, for example: (a) Breslow, D. S.; Heck, R. F. *Chem. Ind. (London)* **1960**, 467. (b) Schwartz, J.; Cannon, J. B. *J. Am. Chem. Soc.* **1974**, *96*, 2276–2278. (c) Bergman, R. G. *Acc. Chem. Res.* **1980**, *13*, 113–120. (d) Nappa, M. J.; Santi, R.; Diefenbach, S. P.; Halpern, J. *J. Am. Chem. Soc.* **1982**, *104*, 619–621. (e) Tam, W.; Wong, W. K.; Gladysz, J. A. *Ibid.* **1979**, *101*, 1589–1591.

(22) See, for example: (a) Berry, M.; Elmitt, K.; Green, M. L. H. *J. Chem. Soc., Dalton Trans.* **1979**, 1950–1958. (b) Rest, A. J.; Whitwell, I.; Graham, W. A. G.; Hoyano, J. K.; McMaster, A. D. *J. Chem. Soc., Chem. Commun.* **1984**, 624–625.

The thermolyses of labeled cyclohexyl complexes **1-d₁** and **1-d₁₂** in benzene provide the only mechanistic observations which are not easily accommodated by mechanism a. In particular, the inverse isotope effect, $k_1/k_{1-d_{12}} = 0.7 \pm 0.1$, is hard to reconcile with a simple reductive elimination mechanism.²⁴ Theoretically, an inverse kinetic isotope effect as low as 0.7 can arise from a single, very endothermic, elementary step if that step proceeds from a starting material with hydrogen weakly bound to a product with hydrogen strongly bound via a very product-like transition state.²⁵ It is conceivable that these criteria could be met by reductive elimination from **1** to form Cp*PMe₃Ir and free cyclohexane. Such an interpretation, however, would contrast sharply with the normal isotope effects in the range 2.2–3.3 measured for mononuclear, rate-determining alkane reductive elimination from other hydridoalkylmetal complexes.^{20a,b,23} The only inverse isotope effects reported for reductive eliminations from L_nM(R)(H)²⁶ systems are for cases in which R = aryl.²⁷ In these cases, an inverse effect has been explained not as a kinetic isotope effect but as an equilibrium isotope effect arising from an equilibrium between the hydridoaryl complex and an η²-arene complex prior to complete dissociation of arene. To rationalize our inverse effect as an equilibrium effect requires an intermediate between cyclohexyl complex **1** and Cp*PMe₃Ir plus cyclohexane. We propose that a σ-complex (Scheme IV) might be such an intermediate; the rate acceleration observed for **1-d₁₂** relative to **1** can be thought to arise from a higher steady state concentration of this species. We envision a nearly fully formed C–H bond in the σ-complex and an M–C–H interaction of the type found in agostic M–C–H interactions.²⁸ Such a structure may be considered a C–H analogue of recently discovered nondissociatively bound H₂ complexes.²⁹ Complexes between alkanes and coordinatively unsaturated metal centers have been postulated in matrix-isolation studies.³⁰ Although this type of interaction has been substantiated in the chelated ligands of isolated, structurally characterized species, we believe that the observations described here constitute the first empirical evidence for the intermediacy of σ-complexes in alkane reductive elimination.^{31,32}

A σ-complex intermediate could also provide an explanation for the hydride-to-α-cyclohexyl scrambling observed on thermolysis of **1-d₁**. As illustrated in Scheme V, the iridium center in the



$$D_{\text{Ir-cy}} + D_{\text{Ir-H}} \approx 95 + 35 - 5 = 125 \text{ kcal/mol}$$

Figure 6. Proposed approximate reaction coordinate diagrams for the reaction of **1** with benzene. The solid and dashed lines represent respectively mechanism a (Scheme IIIa) and the σ-complex mechanism (Scheme IV).

σ-complex could migrate from complexation with the α-C–D bond to complexation with the α-C–H bond; this isomerization could be followed by a chair–chair flip and insertion into the (now equatorial) C–H bond to give **1-α-d₁**.³³ This is one explanation for the scrambling process. We acknowledge that the scrambling need not involve intermediates along the reaction coordinate for the conversion of **1** to **2**, and one can imagine side reactions (notably α-elimination³⁴ and reinsertion or a concerted dyatropic rearrangement³⁵) which could also affect the scrambling. In any case, it is interesting that scrambling appears to be confined to the α-position, so the iridium center does not migrate around the cyclohexyl ring.

In conclusion, the experimental data are consistent with mechanism a or a variant thereof with a σ-complex intermediate on the pathway to reductive elimination of cyclohexane. We cannot kinetically distinguish between these possibilities, but either one allows us to interpret further two aspects of our kinetic data: inhibition of the reaction by cyclohexane and the magnitude of ΔH[‡]. From the slope and intercept of the plot in Figure 4b, the quantity $k_2/k_{-1} = 2.5$ may be calculated. This represents the kinetic selectivity of the Cp*PMe₃Ir intermediate and implies that there is a 2.5-fold kinetic preference of the intermediate for reaction with benzene compared to cyclohexane. Considering the much greater thermodynamic stability of the benzene oxidative addition product, the kinetic selectivity is remarkably low and presumably reflects the high reactivity of Cp*PMe₃Ir. Note also that the 2.5-fold kinetic selectivity at 130 °C is consistent with the 4.0-fold selectivity observed in photolyses of Cp*(PMe₃)Ir(H)₂ in benzene–cyclohexane mixtures at 8 °C,^{1k} the discrepancy being attributable to the difference in temperatures. These values suggest that the same intermediate is involved in the thermal and photochemical C–H activation reactions.

The value of ΔH[‡] provides information about the combined strengths of the iridium–cyclohexyl and iridium–hydride bond in **1**. As illustrated in Figure 6, the sum of these energies must be equal to the cyclohexane C–H bond strength (95.5 kcal/mol),¹⁷ plus the enthalpy of activation for cyclohexane elimination (35 kcal/mol), less the enthalpy of activation for cyclohexane oxidative addition to Cp*PMe₃Ir. On the basis of the low kinetic selectivity of the intermediate and preliminary laser flash photolysis experiments,³⁶ we estimate that the latter quantity is less than or equal to 5 kcal/mol, suggesting that the sum of the Ir–H and Ir–C

(24) The isotope effect measured is admittedly a composite of primary and secondary effects, but the contribution of the secondary effect is expected to be negligible because the α-carbon hybridization is sp³ in both **1** and free cyclohexane.

(25) While theoretical treatments, such as Bigeleisen's, predict the possibility of inverse kinetic isotope effects, Melander and Saunders have argued that there is no experimental evidence for such effects. (a) Bigeleisen, J. *Pure Appl. Chem.* **1983**, *8*, 217–223. (b) Melander, L.; Saunders, W. H. "Reaction Rates of Isotopic Molecules"; Wiley-Interscience: New York, 1980; pp 157–158.

(26) Significant inverse isotope effects have been observed for reductive elimination of dihydrogen from L_nMH₂ complexes. See: Howarth, O. W.; McAteer, H. H.; Moore, P.; Morris, G. E. *J. Chem. Soc., Dalton Trans.* **1984**, 1171–1180 and references therein.

(27) (a) Jones, W. D.; Feher, F. J. *J. Am. Chem. Soc.* **1985**, *107*, 620–631. (b) Feher, F. J. Ph.D. Thesis, University of Rochester, New York, 1984.

(28) Brookhart, M.; Green, M. L. H. *J. Organomet. Chem.* **1983**, *250*, 395–408. For interactions in which a ligand is bound to the metal by only an M–C–H interaction, the term "agostic" (from the Greek αγοςγω, to clasp or hold oneself) seems inappropriate. By analogy to a π-complex of an olefin, we prefer σ-complex as a general term to describe a three center, two electron bonding interaction between a metal and an organic σ-bond.

(29) (a) Kubas, G. J.; Ryan, R. R.; Swanson, B. I.; Vergamini, P. J.; Wasserman, H. J. *J. Am. Chem. Soc.* **1984**, *106*, 451–452. (b) Upmacis, R. K.; Gadd, G. E.; Poliakoff, M.; Simpson, M. B.; Turner, J. J.; Whyman, R.; Simpson, A. F. *J. Chem. Soc., Chem. Commun.* **1985**, 27–30. (c) Church, S. P.; Grevels, F.-W.; Herrmann, H.; Schaffner, K. *Ibid.* **1985**, 794–795.

(30) See, for example: ref 29c and Poliakoff, M.; Turner, J. J. *J. Chem. Soc., Dalton Trans.* **1974**, 2276.

(31) In ab initio calculations on the M(CH₃)(H) → M + CH₄ (M = Pd, Pt) reaction surface, Low and Goddard identify energy minima corresponding to methane σ-complexes in which more than one C–H bond simultaneously interacts with the metal. However, the binding energy of methane in these species is estimated to be only a few kcal/mol. See ref 4a.

(32) A similar explanation was recently invoked to explain an inverse isotope effect observed for isomerization of [Cp₂W(H)(CH₂PMe₂Ph)]⁺ to [Cp₂W(CH₃)(PMe₂Ph)]⁺: Green, J. C.; Green, M. L. H.; Morley, C. P. *Organometallics* **1985**, *4*, 1302–1305.

(33) Scheme V is based on the assumption that insertion of the iridium center into the equatorial C–H bond occurs more rapidly than insertion into the axial C–H bond. This need not be true. If these two insertions were competitive, the α-scrambling could occur from the first σ-complex intermediate by sequential axial insertion and ring inversion.

(34) (a) Schrock, R. R. *J. Am. Chem. Soc.* **1975**, *97*, 6577–6578. (b) Cooper, J. J.; Green, M. L. H. *J. Chem. Soc., Chem. Commun.* **1974**, 761–762. (c) Thorn, D. L. *Organometallics* **1985**, *4*, 192–194.

(35) Erker, G. *Acc. Chem. Res.* **1984**, *17*, 103–109.

(36) Nazran, O.; Griller, D., unpublished results.

bond dissociation enthalpies (BDE's) is approximately 135 kcal/mol. This requires that if the M-H BDE is the roughly 60–65 kcal/mol normally estimated,³⁷ the M-C BDE must be unusually high, perhaps as large as 75 kcal/mol.³⁸ Alternatively, if the Ir-H bond energy is as high as the 78 kcal/mol which has been estimated³⁹ for $\text{H}_2\text{Os}(\text{CO})_4$, the Ir-C BDE could be correspondingly lower (60–65 kcal/mol). In any case, it is certain that either or both of the metal-alkyl and metal-hydrogen bond energies must exceed all previous estimates for late transition-metal systems. These bond energies emphasize the special thermodynamic driving force for C-H activation in this system.

Thermodynamic Experiments. Information about the absolute or relative strengths of metal-carbon bonds in organo-transition-metal complexes typically has been derived from three methods:⁴⁰ thermochemical, kinetic, and thermodynamic. Each method represents a different approach to the determination of ΔH° for a reaction in which the bond of interest is formed or broken; absolute or relative bond energies are then deduced from the value of ΔH° and knowledge of the strengths of the other bonds that are broken or formed in the reaction. The method described here is a variation of the thermodynamic approach described by Halpern.^{40,41} It is also qualitatively similar to the approaches of Applequist and O'Brien to the study of equilibria in halogen-lithium interconversions⁴² and of Marcomini and Poë to the determination of metal-metal bond strengths in $\text{M}_2(\text{CO})_{10}$ dimers (M = Mn, Re).⁴³

That an equilibrium method could be applied to the study of hydrocarbon reductive eliminations and oxidative additions indicates the remarkable reversibility of this C-H activation system. Clearly, dimerization or other side reactions of the $\text{Cp}^*\text{PMe}_3\text{Ir}$ intermediate must be kinetically or thermodynamically unfavorable relative to insertion into C-H bonds. Also, reductive elimination of alkane from the hydrido alkyl complexes must be highly kinetically favorable relative to β -elimination or other reactions which would drain iridium from the equilibria (β -elimination may be responsible for the slow formation of $\text{Cp}^*(\text{PMe}_3)_2\text{Ir}(\text{H})_2$ under equilibration conditions¹⁴).

The equilibration method suffers from several disadvantages which limit its utility. There are practical problems associated with studying equilibria involving methane, ethane, and other highly volatile hydrocarbons. Also difficult to study are equilibria with highly unsymmetrical hydrocarbons (those with several different kinds of C-H bonds). Finally, the use of NMR integrations to determine relative amounts of hydrido alkyl complexes at equilibrium limits one to the determination of K_{eq} values in the range $0.005 < K_{\text{eq}} < 200$, corresponding to only about an 8-kcal/mol range of ΔG° values. This range can, however, be extended by establishing a ladder of hydrido alkyl complex stabilities.

Despite limitations of the method, a qualitative trend in the strengths of the following iridium-alkyl bonds was discerned (Table V): neopentyl < cyclohexyl \sim cyclopentyl < primary 2,3-dimethylbutyl < primary pentyl. Note that the strongest Ir-R bonds are formed by breaking strong C-H bonds. This reactivity pattern (reflecting $D_{\text{M-R}} + D_{\text{M-H}} > D_{\text{R-H}}$) is essential for any alkane activation/functionalization system that attempts to se-

lectively functionalize methane or the primary positions of alkanes. The sample of compounds studied does not permit a detailed analysis of the factors determining iridium-carbon bond strengths in this system, but it is interesting to note that the observed trend could be predicted on the basis of a combination of alkyl radical stabilities and alkyl group steric bulk (the importance of ionic contributions to Ir-R bonding (i.e., $\text{Ir}^+ \text{R}^-$) cannot be assessed for want of reliable data on the electron affinities of the alkyl groups studied⁴⁴). The influence of steric factors is further emphasized by equilibration of the two methyl activation products of 2,2-dimethylbutane (Table IV). Here the two types of C-H bonds are virtually indistinguishable *except* for the difference in repulsive interactions that result from activation of each. Yet the equilibrium favors ($K_{\text{eq}} > 20$) activation of the least sterically encumbered methyl group.

The iridium-phenyl bond appears to be over 25 kcal/mol stronger than the iridium-cyclohexyl bond, and the stability of the hydrido phenyl complex **2** precluded its equilibration with any of the hydrido alkyl complexes. The origin of this stability is not clear, although it is consistent with differences in radical stabilities¹⁷ and electron affinities⁴⁴ between the phenyl radical and alkyl radicals. Whatever the origin of the high Ir-Ph bond strength, the figures $D_{\text{Ir-Ph}} - D_{\text{Ir-Cy}} \geq 20$ kcal/mol and $D_{\text{Ir-Cy}} + D_{\text{Ir-H}} \geq 135$ kcal/mol suggest that $D_{\text{Ir-Ph}} + D_{\text{Ir-H}} \geq 155$ kcal/mol.

Summary. This work attempts to delineate the mechanism of hydrocarbon exchange at an iridium center and determine relative strengths of iridium-carbon bonds in several hydrido alkyl complexes. The exchange mechanism, as studied in the case of the conversion of hydrido cyclohexyl complex **1** to hydrido phenyl complex **2** in benzene, appears to proceed by reductive elimination of one hydrocarbon followed by oxidative addition of the other. Two results, an inverse isotope effect of 0.7 for reductive elimination of cyclohexane and H/D scrambling between the hydride and α -cyclohexyl position of **1**, suggest the possibility of a σ -complex intermediate between **1** and $\text{Cp}^*\text{PMe}_3\text{Ir}$ plus cyclohexane. Kinetic data also permit the estimation of a lower limit for the combined absolute strengths of the iridium-cyclohexyl and iridium-hydride bonds, $D_{\text{Ir-Cy}} + D_{\text{Ir-H}} \geq 135$ kcal/mol.

The equilibration of hydrido alkyl complexes in alkane mixtures gave rise to the following qualitative trend of iridium-carbon bond dissociation energies: neopentyl < cyclohexyl \sim cyclopentyl < primary 2,3-dimethylbutyl < primary pentyl \ll phenyl.

The $\text{Cp}^*\text{PMe}_3\text{Ir}$ system appears to be distinguished from other systems by the thermodynamic favorability of its C-H activation reactions. This observation is in accord with the conclusion of Halpern that "thermodynamic constraints are of dominant importance in limiting the reactivities of metal complexes toward C-H bonds".^{37a} While necessary, thermodynamic favorability appears not to be sufficient to observe the direct product of alkane oxidative addition to an unsaturated metal fragment. In a few cases, at least, the apparent generation of reactive coordinatively unsaturated intermediates (e.g., $\text{Os}(\text{CO})_4$, $\text{CpRe}(\text{CO})_2$) leads to dimer or oligomer rather than C-H addition, despite the probable stability of insertion products (e.g., $(\text{CO})_4\text{Os}(\text{R})(\text{H})$; $\text{Cp}(\text{CO})_2\text{Re}(\text{R})(\text{H})$) to the reaction conditions.⁴⁵⁻⁴⁷ Thus there may be significant kinetic barriers to C-H oxidative addition in some systems.

Experimental Section

General. All reactions were carried out under a nitrogen or argon atmosphere with use of Schlenk techniques or a drybox. Drybox manipulations were performed in a nitrogen-filled Vacuum Atmospheres 553-2 drybox with attached M6-40-1H Dri-train. ¹H NMR spectra were recorded on a Bruker AM 500 or the 200-, 250-, and 300-MHz spectrometers constructed at the University of California at Berkeley (UCB) NMR facility. ²H NMR, ¹³C NMR, and ³¹P NMR spectra were recorded on a Bruker AM 500 or the UCB 300-MHz spectrometer. ¹H NMR, ²H NMR, and ¹³C NMR chemical shifts are reported in parts per million downfield of tetramethylsilane (tetramethylsilane-*d*₁₂). ³¹P NMR chemical shifts are reported in ppm downfield of 85% H₃PO₄. All cou-

(37) (a) Halpern, J. *Inorg. Chim. Acta* **1985**, *100*, 41-48. (b) Pearson, R. G. *Chem. Rev.* **1985**, *85*, 41-49.

(38) In soluble transition-metal complexes, metal-hydride bonds are usually much stronger than metal-alkyl bonds (for an apparent exception, see ref 2e). However, most accurate data on BDEs (as opposed to average bond enthalpies) are available for first-row metals, and third-row M-C bonds are undoubtedly much stronger. The opposite ($D_{\text{M-C}} > D_{\text{M-H}}$) has been found for hydrogen and carbon bonds to naked metal ions. (a) Armentrout, P. B.; Halle, L. F.; Beauchamp, J. L. *J. Am. Chem. Soc.* **1981**, *103*, 6501-6502. (b) Mandich, M. L.; Halle, L. F.; Beauchamp, J. L. *Ibid.* **1984**, *106*, 4403-4416 and references therein.

(39) Calderazzo, F. *Ann. N. Y. Acad. Sci.* **1983**, *415*, 37. We are grateful to Prof. J. Norton for calling this estimate to our attention.

(40) Halpern, J. *Acc. Chem. Res.* **1982**, *15*, 238-244.

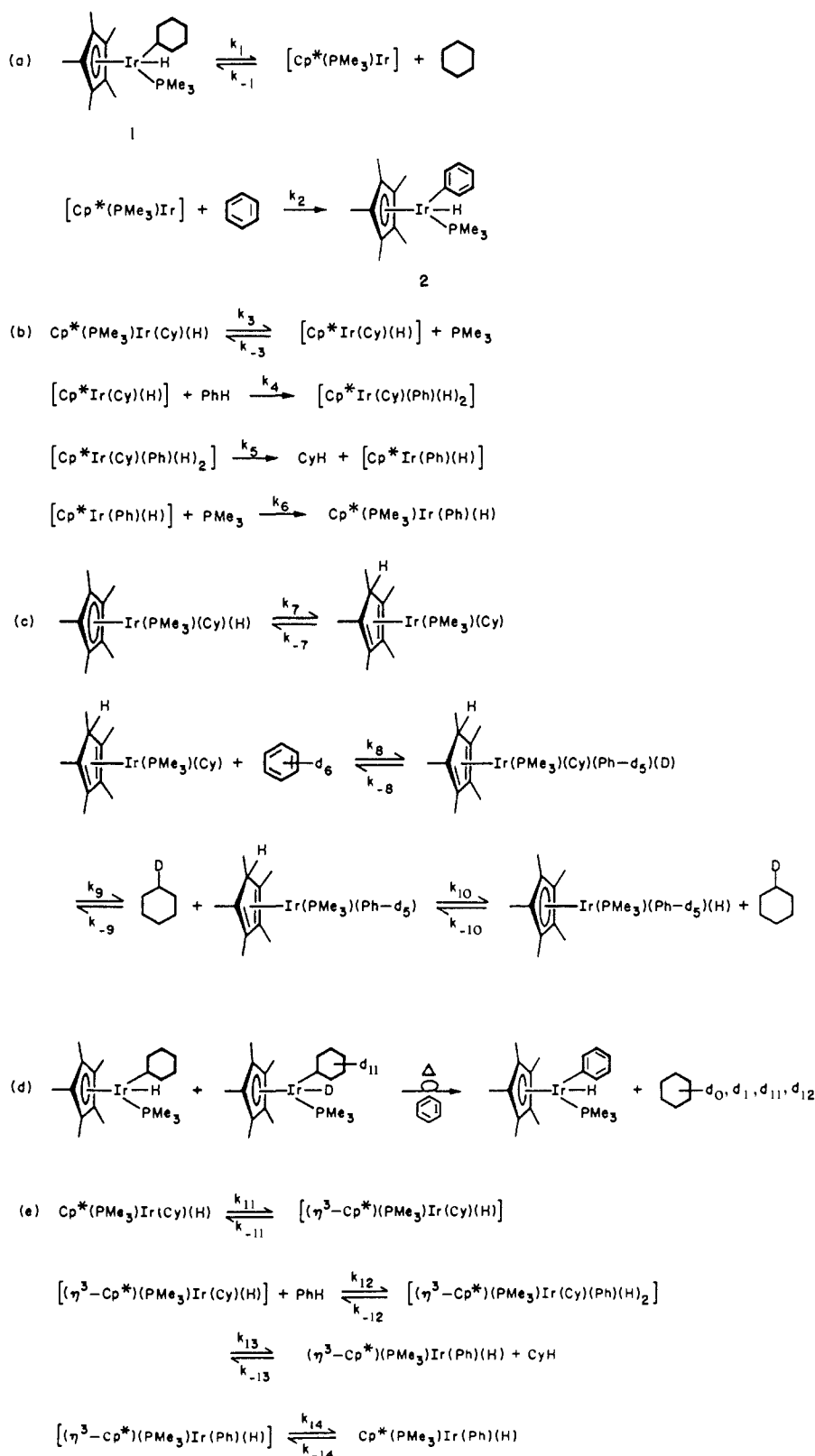
(41) Halpern, J. *Pure Appl. Chem.* **1979**, *51*, 2171-2182.

(42) Applequist, D. E.; O'Brien, D. F. *J. Am. Chem. Soc.* **1963**, *85*, 743-748.

(43) Marcomini, A.; Poë, A. *J. Chem. Soc., Dalton Trans.* **1984**, 95-97.

(44) Depuy, C. H.; Bierbaum, V. M.; Damrauer, R. *J. Am. Chem. Soc.* **1984**, *106*, 4051-4053.

Scheme III

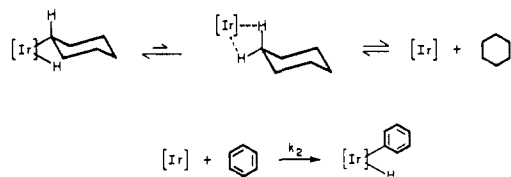


pling constants are reported in Hz. Infrared spectra were recorded on a Perkin-Elmer 283 grating spectrometer or a Perkin-Elmer 1550 Fourier transform spectrometer. Melting points (uncorrected) were determined with a Thomas-Hoover capillary melting point apparatus. Elemental analyses were conducted by the UCB microanalytical laboratory, and mass spectra were recorded by the UCB mass spectrometry laboratory.

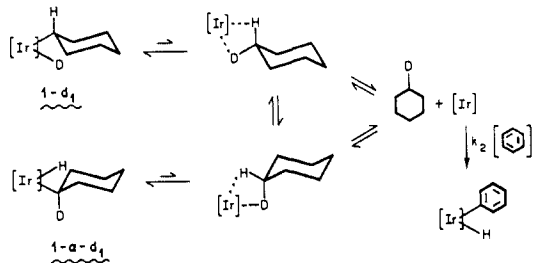
Unless otherwise noted, reagents and solvents were used as received from commercial suppliers. Lithium borohydride and sodium borodeuteride (98% D) were purchased from Alfa and Aldrich, respectively; neopentane (2,2-dimethylpropane) was obtained from Pfaltz and Bauer;

methyl lithium was purchased from Fluka AG; anilinium hydrochloride was purchased from Aldrich and recrystallized from methanol/diethyl ether before use; methyl- d_3 iodide was purchased from Cambridge Isotope Laboratories; lithium metal was purchased from Lithcoa. Benzene, benzene- d_6 , and diethyl ether were distilled under nitrogen from sodium-benzophenone. Cyclohexane and cyclohexane- d_{12} were washed first with concentrated H_2SO_4 then with water and aqueous Na_2CO_3 before predrying over MgSO_4 and distillation under nitrogen from CaH_2 . Pentane, hexane, 2,3-dimethylbutane, and 2,2-dimethylbutane were distilled from CaH_2 under nitrogen. Trimethylphosphine and tri-

Scheme IV



Scheme V



phenylphosphine were purchased from Strem; the former was vacuum transferred from Na/K alloy, and the latter was recrystallized from hexane prior to use. $\text{Cp}^*(\text{PMe}_3)\text{IrCl}_2^{13}$ and $\text{Cp}^*(\text{PMe}_3)\text{Ir}(\text{H})_2^{1k}$ were prepared by literature methods.

"Pyrex bomb" denotes a 50-mL cylindrical vessel of medium-wall Pyrex glass sealed to a high-vacuum Teflon stopcock.

Preparative Photolyses. The photolysis apparatus consisted of a 450-W Canrad-Hanovia mercury immersion lamp with an Ace 7830-60 power supply and an Ace 7874B-38 immersion well. The immersion well was secured in a Dewar flask filled with water cooled to 5–10 °C by a Lauda K-4/RD refrigerated bath circulator. In a typical photolysis, $\text{Cp}^*(\text{PMe}_3)\text{Ir}(\text{H})_2$ (200–500 mg) was dissolved in approximately 25–50 mL of the appropriate hydrocarbon in a Pyrex bomb. The solution was irradiated for about 12 h during which time the color of the solution turned from clear to brown. Solvent was removed under vacuum and the brown oily residue was purified by cold chromatography (alumina III, 15 cm \times 3 cm diameter; 6% diethyl ether/hexane) to yield analytically pure material. Cold chromatography was performed under nitrogen outside the drybox with a double-jacketed glass column. Nitrogen was bubbled through liquid nitrogen and then circulated through the inner jacket to maintain the column temperature at about –80 °C, as independently verified by a thermocouple inserted into the alumina III support under chromatography conditions.

Equilibrations. Equilibrations were conducted in a factory-calibrated Neslab Exacal EX-250HT high-temperature bath filled with Dow Corning 210H silicone fluid, whose temperature was checked with a calibrated Omega DSS-199-P2-OC platinum resistance digital thermometer. Hydrocarbon mixtures were prepared in about 50-mL portions by weighing each component after it was added to a stoppered volumetric flask. NMR sample tubes with a minimum gas-phase volume were used to maintain the solvent composition nearly constant between room temperature and 140 °C (Figure 5). Samples were prepared by dissolving approximately 10 mg of hydrido alkyl complex in a hydrocarbon mixture in a medium-wall Wilmad 504PP NMR tube. The tube was flame-sealed under vacuum after positioning the 3-mm glass rod so as to displace all but about 0.3 mL of room-temperature gas-phase volume (this allowed for liquid-phase expansion on heating to 140 °C). Samples were excluded from room light. Progress of the equilibration was monitored by ^{31}P NMR, and when a stable ratio of hydrido alkyl complexes was obtained, that ratio was evaluated by ^{31}P NMR, using a delay of at least ten times the longest spin-lattice relaxation time (T_1) between pulses.

Kinetics. Samples were flame-sealed under vacuum in 5-mm NMR tubes, heated in the Neslab high-temperature bath described above, and cooled quickly to 0 °C in ice water after being removed from the bath. The reactions were typically monitored to greater than 3 half-lives by ^1H NMR at room temperature by integrating either the hydride resonances

Table VI. Crystal and Data Collection Parameters for 1

Compound: $\text{Ir}(\text{H})(\text{C}_6\text{H}_{11})(\text{C}_5(\text{CH}_3)_5)(\text{P}(\text{CH}_3)_3)$	
(A) Crystal Parameters at 25 °C ^{a,b}	
$a = 13.1549$ (18) Å	space group: $P2_1/n$
$b = 18.6520$ (19) Å	formula weight = 487.67 amu
$c = 17.2996$ (14) Å	$Z = 8$
$\beta = 107.127$ (8)°	$d_c = 1.60$ g cm ⁻³
$V = 4055.8$ (15) Å ³	$\mu(\text{calcd}) = 66.32$ cm ⁻¹
size of crystal: 0.20 \times 0.22 \times 0.28 mm	
(B) Data Measurement Parameters	
radiation: Mo K α ($\lambda = 0.71073$ Å)	
monochromator: highly-oriented graphite ($2\theta = 12.2^\circ$)	
detector: crystal scintillation counter, with PHA	
reflections measured: $\pm h, +k, +l$	
2θ range: 3° \rightarrow 53°	scan type: θ - 2θ
scan speed: 0.60 \rightarrow 6.7 (θ , deg/min)	
scan width: $\Delta\theta = 0.5 \pm 0.35 \tan \theta$	
background: measured over 0.25($\Delta\theta$) added to each end of the scans	
aperture \rightarrow crystal = 173 mm vertical aperture = 3.0 mm	
horizontal aperture = 2.0 + 1.0 $\tan \theta$ (mm) (variable)	
no. of reflections collected: 9103	
no. of unique reflections: 8394	
intensity standards: (486), (3511), (866); measured every 2 h of X-ray exposure time; over the data collection period a 9.8% decrease in intensity was observed	
orientation: 3 reflections were checked after every 250 measurements; crystal orientation was redetermined if any of the reflections were offset from their predicted positions by more than 0.1°; reorientation was done twice during data collection	

^a Unit cell parameters and their esd's were derived by a least-squares fit to the setting angles of the unresolved Mo K α components of 24 reflections with 2θ near 28°. ^b The esd's of all parameters are given in parentheses, right-justified to the least significant digit(s) given.

or the trimethylphosphine resonances of cyclohexyl complex 1 and phenyl complex 2 vs. an external standard ($(\text{C}_5\text{H}_5)\text{Ir}(\text{PMe}_3)(\text{H})_2^{48}$ provided a convenient standard in the hydride region, while hexamethylsiloxane was used for the alkyl region of the spectrum). Delays between pulses of at least ten times the longest proton T_1 were used.

$\text{Cp}^*(\text{PMe}_3)\text{Ir}(\text{Cy})(\text{H})$ (1- d_1). Photolysis of $\text{Cp}^*(\text{PMe}_3)\text{Ir}(\text{H})_2$ in cyclohexane, followed by cold chromatography, as described above, gave a 52% yield of product: mp 74.5–75.5 °C; IR (C_6D_6) 2098 (s) cm⁻¹, $\nu_{\text{Ir-H}}$; ^1H NMR (C_6D_6) δ 2.32 (m, 1 H, α -CH), 2.20–1.53 (m, β , β' , γ , γ' , δ -CHH'), 1.87 (dd, $J = 1.8, 0.7$, $\text{C}_5(\text{CH}_3)_5$), 1.24 (d, $J = 9.5$, $\text{P}(\text{CH}_3)_3$), –18.68 (d, $J = 37.0$, Ir-H); $^{13}\text{C}\{^1\text{H}\}$ NMR (C_6D_6) δ 92.36 (d, $J = 3.4$, C_5Me_5), 44.58 (d, $J = 4$, β -CHH'), 43.96 (d, $J = 2$, β' -CHH'), 32.92 (s, γ -CHH'), 32.85 (s, γ' -CHH'), 28.33 (s, δ -CHH'), 19.69 (d, $J = 35.7$, $\text{P}(\text{CH}_3)_3$), 10.75 (s, $\text{C}_5(\text{CH}_3)_5$), 3.26 (d, $J = 7.4$, α -CH); $^{31}\text{P}\{^1\text{H}\}$ NMR (C_6D_6) δ –44.9; MS, m/e 487/485. Anal. Calcd for $\text{C}_{19}\text{H}_{36}\text{IrP}$: C, 46.79; H, 7.44. Found: C, 47.05; H, 7.65.

$\text{Cp}^*(\text{PMe}_3)\text{Ir}(\text{Cy})(\text{D})$ (1- d_1). A 100-mL Schlenk flask equipped with stirbar and septum was charged with $\text{Cp}^*(\text{PMe}_3)\text{Ir}(\text{Cy})(\text{Br})^{1k}$ (85 mg, 150 μmol) and NaBD_4 (38 mg, 910 μmol). Argon-saturated isopropyl alcohol (30 mL) was added via cannula, and the resulting yellow solution was stirred at room temperature for 14 h, during which time the solution gradually turned colorless. Volatile materials were removed under vacuum and the residue was extracted with toluene. On concentration, the toluene extract yielded 70 mg (95%) of product: IR (C_6H_6) 1508 (m) cm⁻¹; ^2H NMR (C_6H_6) δ –18.49 (d, $J = 5$, Ir-D); $^{31}\text{P}\{^1\text{H}\}$ NMR (C_6D_6) δ –44.6 (t, $J = 5$).

$\text{Cp}^*(\text{PMe}_3)\text{Ir}(\text{Cy}-d_{11})(\text{D})$ (1- d_{12}). A cyclohexane- d_{12} (40 mL) solution of $\text{Cp}^*\text{Ir}(\text{PMe}_3)_2(\text{H})_2$ (323 mg, 0.797 mmol) in a Pyrex bomb was irradiated for 13.7 h and then heated at 150 °C for 55 min.⁵⁰ Cold chromatography afforded 165 mg (41%) of product: IR (C_6H_6) 1508 (m) cm⁻¹; ^2H NMR (C_6H_6) δ 2.20 (m, α -CD), 2.08–1.43 (m, β , β' , γ , γ' , δ -CDD'), –18.51 (d, $J = 5$, Ir-D); $^{31}\text{P}\{^1\text{H}\}$ NMR (C_6D_6) δ –44.5 (t, $J = 5$).

(45) $\text{Os}(\text{CO})_4(\text{CH}_3)(\text{H})$,^{20a,46} $\text{Os}(\text{CO})_4(\text{CH}_2\text{CH}_3)(\text{H})$,⁴⁶ and $\text{CpRe}(\text{CO})_2(\text{CH}_2\text{C}_6\text{H}_5)(\text{H})$ ^{4a} are all known compounds with at least marginal stability at room temperature.

(46) Carter, W. J.; Kelland, J. W.; Okrasinski, S. J.; Warner, K. E.; Norton, J. R. *Inorg. Chem.* **1982**, *21*, 3955–3960.

(47) Perutz and co-workers generated $\text{CpRe}(\text{CO})_2$ from photolysis of $\text{CpRe}(\eta^2\text{-C}_3\text{H}_6)(\text{CO})_2$ in methane matrices at 17–20 K but saw no evidence for methane oxidative addition to form $\text{CpRe}(\text{CO})_2(\text{CH}_3)(\text{H})$ at this temperature. Chetwynd-Talbot, J.; Grebenik, P.; Perutz, R. N.; Powell, M. H. A. *Inorg. Chem.* **1983**, *22*, 1675–1678.

(48) This complex is stable to extended heating in benzene at 150 °C. Its synthesis and chemistry will be reported separately: mp 121–122 °C; IR (C_6H_6) 2139 (s) cm⁻¹; ^1H NMR (C_6D_6) δ 5.03 (s, C_5H_5), 1.37 (d, $J = 10.7$ Hz, $\text{P}(\text{CH}_3)_3$), –17.47 (d, $J = 13.3$ Hz, Ir-H); $^{13}\text{C}\{^1\text{H}\}$ NMR (C_6D_6) δ 78.34 (d, $J = 2.0$ Hz, C_5H_5), 26.58 (d, $J = 38.5$ Hz, $\text{P}(\text{CH}_3)_3$); $^{31}\text{P}\{^1\text{H}\}$ NMR (C_6D_6) δ –42.3; MS, m/e 336/334. Anal. Calcd for $\text{C}_8\text{H}_{16}\text{IrP}$: C, 28.65; H, 4.81. Found: C, 28.83; H, 4.89.

(49) Previously reported (ref 1k) and characterized spectroscopically; fully characterized after conversion to the corresponding bromide, $\text{Cp}^*(\text{PMe}_3)\text{Ir}(\text{R})(\text{Br})$.

X-ray Data Collection, Structure Determination, and Refinement for Cp*(PMe₃)Ir(Cy)H (1). Pale yellow columnar crystals of the compound were obtained by slow crystallization from concentrated pentane solution cooled to -40 °C. The crystalline material is relatively insensitive to atmospheric oxygen and water. Fragments cleaved from some of the crystals were mounted in capillaries in air and the capillaries flushed with dry nitrogen and then flame sealed. Preliminary precession photographs indicated monoclinic Laue symmetry and yielded preliminary cell dimensions. Systematic absences were consistent only with space group $P2_1/n$.

The crystal used for data collection was then transferred to our Enraf-Nonius CAD-4 diffractometer⁵¹ and centered in the beam. Automatic peak search and indexing procedures yielded the monoclinic reduced primitive cell. Inspection of the Niggli values revealed no conventional cells of higher symmetry. The final cell parameters and specific data collection parameters are given in Table VI.

The 9032 ray intensity data were converted to structure factor amplitudes and their esd's by correction for scan speed, background, and Lorentz and polarization effects. Inspection of the intensity standards showed a monotonic isotropic decrease to 0.9 of the original intensity. The data were corrected for this decay. Inspection of the azimuthal scan data showed a variation $I_{\min}/I_{\max} = 0.63$ for the average curve. The data were corrected for absorption by using this empirical curve. Removal of systematically absent and redundant data left 8394 unique data.

The structure was solved by Patterson methods with use of only the low-angle ($\sin \Phi/\lambda < 0.54$) data to reveal the two unique molecules in the unit cell. The structure was refined via standard least-squares and Fourier techniques with use of all the data. In a difference Fourier map calculated following refinement of all non-hydrogen atoms with anisotropic thermal parameters, peaks corresponding to the expected positions of most of the hydrogen atoms were found. The hydrogens were included in the structure factor calculations in their expected positions based on idealized bonding geometry and were then refined in least squares with isotropic thermal parameters. Refinement continued with the inclusion of a secondary extinction parameter and the removal of two low-angle, low-intensity reflections which showed consistently abnormal values of F_{calcd} vs. F_{obsd} .

The final residuals for 668 variables refined against the 6130 data for which $F^2 > 3\sigma(F^2)$ were $R = 2.17\%$, $wR = 2.54\%$, and $\text{GOF} = 1.150$. The R value for all 8392 data was 5.19%. Positional parameters and esd's for heavy atoms and selected hydrogens are given in Table VII.

The quantity minimized by the least-squares program was $\sum w(|F_o| - |F_c|)^2$, where w is the weight of a given observation. The p -factor, used to reduce the weight of intense reflections, was set to 0.03. The analytical forms of the scattering factor tables for the neutral atoms were used and all non-hydrogen scattering factors were corrected for both the real and imaginary components of anomalous dispersion.

Inspection of the residuals ordered in ranges of $\sin \theta/\lambda$, $|F_o|$, and parity and value of the individual indexes showed no unusual features or trends. The largest peak in the final difference Fourier map had an electron density of $1.31 \text{ e}^-/\text{\AA}^3$. All peaks with density greater than $0.5 \text{ e}^-/\text{\AA}^3$ were located within 1 \AA of an iridium atom.

ORTEP⁵² drawings, values of hydrogen positional parameters for both molecules in the asymmetric unit, anisotropic thermal parameters, and a listing of the values of F_o and F_c are available as supplementary material.

Cp*(PMe₃)Ir(Ph)(H) (2).⁴⁹ A benzene (20 mL) solution of Cp*(PMe₃)Ir(H)₂ (480 mg, 1.18 mmol) in a Pyrex bomb was irradiated for 28 h. The crude product was purified by room-temperature chromatography (alumina III, benzene) to give 223 mg (39%) of product: mp 67–68 °C; IR (C₆H₆) 2098 (s) cm⁻¹; ¹H NMR (C₆D₆) δ 7.75 (m, *m*-CH), 7.10 (m, *o*-CH), 7.08 (m, *p*-CH), 1.81 (dd, $J = 1.8, 0.8$, C₅(CH₃)₅), 1.09 (d, $J = 10.0$, P(CH₃)₃), -17.04 (d, $J = 36.8$, Ir-H); ¹³C{¹H} NMR (C₆D₆) δ 145.47 (br s, *o*-C), 136.65 (d, $J = 13.3$, *i*-C), 127.51 (s, *m*-C), 121.16 (s, *p*-C), 92.60 (d, $J = 3.0$, C₅Me₅), 19.07 (d, $J = 38.1$, P(CH₃)₃), 10.48 (s, C₅(CH₃)₅); ³¹P{¹H} NMR (C₆D₆) δ -41.6; MS, m/e 482/480. Anal. Calcd for C₁₉H₃₀IrP: C, 47.38; H, 6.28. Found: C, 47.12; H, 6.54.

Table VII. Positional Parameters and Their Estimated Standard Deviations

atom	<i>x</i>	<i>y</i>	<i>z</i>	<i>B</i> (Å ²)
Ir1	0.21367 (1)	0.11938 (1)	0.26404 (1)	2.529 (3)
Ir2	0.21585 (1)	0.24578 (1)	0.77574 (1)	2.598 (3)
P1	0.1296 (1)	0.19181 (7)	0.16415 (6)	4.00 (3)
P2	0.13524 (9)	0.32729 (6)	0.68520 (6)	3.25 (2)
C1	0.1447 (3)	0.1570 (2)	0.3629 (2)	2.89 (8)
C2	0.2560 (3)	0.1453 (2)	0.3960 (2)	2.97 (8)
C3	0.2775 (3)	0.0708 (2)	0.3872 (2)	3.06 (8)
C4	0.1775 (3)	0.0363 (2)	0.3508 (2)	3.07 (8)
C5	0.0958 (3)	0.0886 (2)	0.3339 (2)	2.94 (8)
C6	0.0868 (3)	0.2247 (2)	0.3677 (3)	4.0 (1)
C7	0.3326 (4)	0.2002 (3)	0.4418 (2)	4.2 (1)
C8	0.3812 (4)	0.0333 (3)	0.4260 (3)	4.3 (1)
C9	0.1614 (4)	-0.0431 (2)	0.3435 (3)	4.3 (1)
C10	-0.0201 (4)	0.0744 (3)	0.3061 (3)	4.7 (1)
C11	0.2392 (4)	0.0474 (2)	0.1764 (2)	3.8 (1)
C12	0.3334 (4)	-0.0021 (3)	0.2102 (3)	4.7 (1)
C13	0.3558 (5)	-0.0511 (3)	0.1446 (3)	7.1 (1)
C14	0.2571 (5)	-0.0930 (3)	0.1010 (3)	7.1 (2)
C15	0.1624 (5)	-0.0458 (3)	0.0673 (3)	6.8 (2)
C16	0.1423 (4)	0.0042 (3)	0.1316 (3)	4.8 (1)
C17	-0.0147 (5)	0.1884 (3)	0.1349 (3)	6.8 (2)
C18	0.1534 (5)	0.1858 (3)	0.0664 (3)	7.0 (2)
C19	0.1581 (6)	0.2868 (3)	0.1841 (4)	8.1 (2)
C21	0.1005 (3)	0.2135 (2)	0.8473 (2)	3.34 (9)
C22	0.1559 (3)	0.2776 (2)	0.8809 (2)	3.37 (9)
C23	0.2656 (3)	0.2629 (2)	0.9103 (2)	3.49 (9)
C24	0.2816 (3)	0.1890 (2)	0.8940 (2)	3.37 (9)
C25	0.1788 (3)	0.1585 (2)	0.8573 (2)	3.24 (9)
C26	-0.0171 (3)	0.2015 (3)	0.8172 (3)	4.6 (1)
C27	0.1026 (4)	0.3464 (3)	0.8939 (3)	4.7 (1)
C28	0.3488 (4)	0.3141 (3)	0.9584 (3)	5.0 (1)
C29	0.3823 (4)	0.1466 (3)	0.9243 (3)	5.1 (1)
C30	0.1561 (4)	0.0800 (2)	0.8428 (3)	4.7 (1)
C31	0.2285 (3)	0.1778 (2)	0.6793 (2)	3.45 (9)
C32	0.1250 (4)	0.1396 (3)	0.6360 (2)	4.1 (1)
C33	0.1350 (4)	0.0933 (3)	0.5651 (3)	5.1 (1)
C34	0.2264 (5)	0.0395 (3)	0.9332 (3)	5.6 (1)
C35	0.3290 (4)	0.0765 (3)	0.6355 (3)	5.3 (1)
C36	0.3183 (3)	0.1233 (3)	0.7057 (2)	4.0 (1)
C37	0.1592 (4)	0.3304 (3)	0.5874 (3)	5.2 (1)
C38	0.1660 (5)	0.4200 (3)	0.7180 (3)	5.6 (1)
C39	-0.0089 (4)	0.3284 (3)	0.6561 (3)	4.8 (1)
H1	0.314 (4)	0.162 (3)	0.263 (3)	8 (1)*
H2	0.320 (3)	0.288 (2)	0.768 (2)	6 (1)*
H11	0.260 (3)	0.073 (2)	0.131 (2)	3.1 (8)*
H31	0.244 (3)	0.217 (2)	0.637 (2)	3.9 (9)*

Molecularity of Cyclohexane Formation. A benzene (2.0 mL) solution of cyclohexyl complexes **1** and **1-d**₁₂ (0.020 M each) and PPh₃ (0.025 M) was heated at 130.0 °C in a Pyrex bomb. At intervals of 1.0, 2.0, 4.4, and 9.0 h, approximately 0.4 mL was removed with a syringe. From each of these portions, volatile materials were transferred into an ampule which was sealed under vacuum and submitted for GC/MS analysis, which indicated that all cyclohexane formed was either *d*₀ or *d*₁₂, with a 10% limit of detection estimated for *d*₁ or *d*₁₁ products. The nonvolatile residue from each portion was redissolved in benzene-*d*₆ and analyzed by ¹H NMR.

Rate Dependence on Benzene Concentration. Four sample tubes with volume-excluding glass rods (see Figure 5) were prepared. Each contained cyclohexyl complex **1** (10 mg, 20 μmol), PPh₃ (5 mg, 20 μmol), an external standard of (C₅H₅)Ir(PMe₃)(H)₂ in benzene, and a mixture of benzene and neopentane. The benzene was added to each tube via syringe, and the neopentane was condensed into the tubes at -196 °C on a vacuum line from a graduated 1-mL Pyrex bomb. The apparatus was then filled with a positive pressure of argon and the upper half of the cajon fitting was loosened long enough to position the glass rod. After reevacuating the apparatus, the sample tubes were flame sealed under vacuum. Solvent compositions, as checked by ¹H NMR, corresponded to benzene mole fractions 0.26 and 0.16. Progress of the reactions was followed by integrating resonances in the hydride region; a frequency modulated presaturation pulse sequence was used to suppress the solvent signals. Reaction rates for each sample were first order in cyclohexyl complex **1** with observed rate constants which were identical within experimental error (Table III, experiment numbers 9–11).

Rate Dependence on Cyclohexane Concentration. Seven samples were prepared as above except that cyclohexane/benzene mixtures (corre-

(50) The initial photolysis product is the desired **1-d**₁₂, but extended irradiation, required for moderate conversion of starting material, leads to significant incorporation of hydrogen atoms in the hydride position of the product. Heating the photolysis mixture exchanges bound cyclohexane with solvent and restores the label in the hydride position.

(51) For a summary of the X-ray diffraction equipment, computational equipment, software, and data reduction formulae used, see: Theopold, K. H.; Bergman, R. G. *Organometallics* **1982**, *1*, 1571. Other details of the X-ray study are supplied as supplementary material.

(52) Johnson, C. K., Report ORNL-3794, Oak Ridge National Laboratory, Oak Ridge, TN, 1965.

sponding to [cyclohexane]/[benzene] = 0, 0.21, 0.42, 0.86, 2.82, 5.20, 10.84) were used and transferred into sample tubes via syringe. The reaction was monitored as above, and observed rate constants are reported in Table I, experiment numbers 12–18.

Cp*(PMe₃)Ir(*n*-pentyl)(H)⁴⁹ An *n*-pentane (50 mL) solution of Cp*(PMe₃)Ir(H)₂ (424 mg, 1.05 mmol) in a Pyrex bomb was irradiated for 36 h. The same solution was heated at 115 °C for 21 h. (Caution: pentane generates a pressure of about 8 atm at this temperature. This procedure should be carried out behind a blast shield or the sashes of a hood.) ³¹P NMR indicated a mixture of 30% dihydride and 70% primary pentyl complex **3**. Purification by cold chromatography gave **3** as a golden oil in 41% yield: IR (C₆H₆) 2096 (s) cm⁻¹; ¹H NMR (C₆D₆) δ 1.88 (d, *J* = 2.0, C₅(CH₃)₅), 1.7–1.3 (m, α, β, γ, δ, CHH'), 1.24 (d, *J* = 9.6, P(CH₃)₃), 1.07 (s, CH₃), -17.81 (d, *J* = 37.3, Ir–H); ¹³C{¹H} NMR (C₆D₆) δ 91.72 (d, *J* = 3.3, C₅Me₅), 41.23 (d, *J* = 1.7, β-CHH'), 39.53 and 23.15 (s, γ, δ-CHH'), 19.23 (d, *J* = 36.2, P(CH₃)₃), 14.75 (d, CH₃), 10.32 (s, C₅(CH₃)₅), -12.10 (d, *J* = 7.1, α-CHH'); ³¹P{¹H} NMR (C₆D₆) δ -43.0; MS, *m/e* 476/474. Anal. Calcd for C₁₈H₃₆IrP: C, 45.45; H, 7.63. Found: C, 45.62; H, 7.64.

Cp*(PMe₃)Ir(2,3-Me₂Bu)(H). This compound was prepared by photolysis and purified by cold chromatography, as above, to give a 60% yield of a one-to-one mixture of two diastereomers which was an oil at room temperature: IR (C₆H₆) 2115 (s) cm⁻¹, both diastereomers; ¹H NMR (C₆D₆) δ 1.854 (d, *J* = 1.5, C₅(CH₃)₅), 1.848 (d, *J* = 1.8, C₅(CH₃)₅), 1.8–1.3 (m, CH₂ and CH), 1.25–1.10 (d, *J* = 6–7, CH₂'s), -17.45 (d, *J* = 36.7, Ir–H), -17.75 (d, *J* = 37.7, Ir–H); ¹³C{¹H} NMR (C₆D₆) δ 91.65 and 91.54 (d, *J* = 3.6, C₅Me₅), 48.17 (br s, β-CH), 46.37 (d, *J* = 2.2, β-CH), 35.43 and 34.87 (s, γ-CH), 21.88 and 21.79 (s, γ-CH₃), 18.87 (d, *J* = 36.5, P(CH₃)₃ both isomers), 18.32 and 17.94 and 17.75 and 17.64 (s, δ-CH₃), 10.35 (s, C₅(CH₃)₅ both isomers), -4.47 and -4.51 (d, *J* = 7.1, α-CH₂); ³¹P{¹H} NMR (C₆D₆) δ -43.0, -43.6; MS, *m/e* 490/488. Anal. Calcd for C₁₉H₃₈IrP: C, 46.60; H, 7.82. Found: C, 46.24; H, 7.93.

Cp*(PMe₃)Ir(neopentyl)(H)^{49,53} This compound was prepared by an analogous route to give a 40% yield of a golden oil: IR (C₆H₆) 2106 (s) cm⁻¹; ¹H NMR (C₆D₆) δ 1.82 (d, *J* = 1.2, C₅(CH₃)₅), 1.72 (d, *J* = 11.9, α-CHH'), 1.53 (dd, *J* = 11.9, 13.1, α-CHH'), 1.29 (s, C(CH₃)₃), 1.21 (d, *J* = 9.6, P(CH₃)₃), -17.78 (d, *J* = 36.5, Ir–H); ¹³C{¹H} NMR (C₆D₆) δ 92.05 (d, *J* = 3.9, C₅Me₅), 35.71 (s, C(CH₃)₃), 33.83 (s, C(CH₃)₃), 19.64 (d, *J* = 37.0, P(CH₃)₃), 10.60 (s, C₅(CH₃)₅), 6.21 (d, *J* = 6.7, Ir–CH₂); ³¹P{¹H} NMR (C₆D₆) δ -43.0; MS, *m/e* 476/474. Anal. Calcd for C₁₈H₃₆IrP: C, 45.45; H, 7.63. Found: C, 45.44; H, 7.70.

Cp*(PMe₃)Ir(cyclopentyl)(H)⁴⁹ This compound was prepared and purified as above to give a 41% yield of golden oil: IR (C₆H₆) 2095 (s) cm⁻¹; ¹H NMR (C₆D₆) δ 2.2–1.5 (m, cyclopentyl CH and CH₂), 1.86 (dd, *J* = 1.8, 0.6, C₅(CH₃)₅), 1.22 (d, *J* = 9.6, P(CH₃)₃), -18.18 (d, *J* = 35.9, Ir–H); ¹³C{¹H} NMR (C₆D₆) δ 92.37 (d, *J* = 3.6, C₅Me₅), 42.42 (d, *J* = 3.5, β-C), 41.37 (s, β'-C), 27.90 (s, γ-C), 27.66 (s, γ'-C), 19.81 (d, *J* = 35.9, P(CH₃)₃), 0.22 (d, *J* = 8.0, α-C); ³¹P{¹H} NMR (C₆D₆) δ -44.83; MS, *m/e* 474/472. Anal. Calcd for C₁₈H₃₄IrP: C, 45.65; H, 7.23. Found: C, 45.56; H, 7.04.

Equilibration of Cp*(PMe₃)Ir(2,2-Me₂Bu)(H) and Cp*(PMe₃)Ir(3,3-Me₂Bu)(H). An otherwise pure binary mixture of products from C–H activation at the two chemically distinct methyl groups of 2,2-dimethylbutane was isolated in 58% yield from photolysis and cold chromatography as above. The mixture was characterized by ¹H NMR, ¹³C NMR, and ³¹P NMR. On heating the mixture for 5 h at 120 °C, the mixture contained >95% of the 3,3-dimethylbutyl isomer, which was identified by its characteristic NMR spectra: ¹H NMR (C₆D₆) δ 1.88 (d, *J* = 2.0, C₅(CH₃)₅), 1.8–1.5 (m, 4 H, α- and β-CHH'), 1.25 (d, *J* = 9.6, P(CH₃)₃), 1.13 (s, C(CH₃)₃), -17.89 (d, *J* = 37.6, Ir–H); ¹³C{¹H} NMR (C₆D₆) δ 91.50 (d, *J* = 26), 56.70 (s, C(CH₃)₃), 33.52 (s, β-CHH'), 29.72 (s, C(CH₃)₃), 19.04 (d, *J* = 36.8, P(CH₃)₃), 10.32 (s, C₅(CH₃)₅), -19.42 (d, *J* = 7.8, α-CHH'); ³¹P NMR {¹H} (C₆D₆) δ -43.1.

Cp*(PMe₃)Ir(CH₃)₂(4). In the drybox, ethereal MeLi (6.0 mL, 1.6 M in Et₂O, low halide, 9.6 mmol) was added in a slow stream to a suspension of Cp*(PMe₃)IrCl₂¹³ (2.0 g, 4.2 mmol) in anhydrous THF (60 mL) at room temperature. The starting material slowly dissolved and after 8 h the yellow solution was filtered through a short pad of alumina(III) and evaporated to dryness. The crude product was taken up in pentane and filtered through a short column of alumina(III) under nitrogen pressure, eluting with additional pentane. The colorless eluent deposited white crystals on slow concentration of the solution in vacuo, affording, after filtration, the dimethyl complex **4** (1.6 g, 88%): mp 67.5–68.5 °C; IR (KBr) 2810 (m), 1230 (m), 1206 (w) cm⁻¹, $\nu_{\text{Ir-CH}_3}$; ¹H NMR (C₆D₆) δ 1.63 (d, *J* = 1.7, C₅(CH₃)₅), 1.05 (d, *J* = 9.4, P(CH₃)₃),

0.42 (d, *J* = 5.9, Ir–CH₃); ¹³C {¹H} NMR (C₆D₆) δ 90.83 (d, *J* = 4.4, C₅Me₅), 14.20 (d, *J* = 35.3, P(CH₃)₃), 8.85 (s, C₅(CH₃)₅), -24.22 (d, *J* = 8.8, Ir–CH₃). Anal. Calcd for C₁₃H₃₀IrP: C, 41.55; H, 7.00. Found: C, 41.71; H, 7.30.

Cp*(PMe₃)Ir(CD₃)₂(4-*d*₆). This compound was prepared by the procedure as above, except that CD₃Li, prepared from CD₃I and Li metal, was used: IR (KBr) 2180 (s), 2106 (m), 2057 (s) cm⁻¹, $\nu_{\text{Ir-CD}_3}$; ¹H NMR (C₆D₆) δ 1.63 (d, *J* = 1.5, C₅(CH₃)₅), 1.04 (d, *J* = 9.5, P(CH₃)₃); ²H NMR (C₆H₆) δ 0.30 (br s, Ir–CD₃).

Cp*(PMe₃)Ir(CH₃)Cl (5) by Ligand Interchange. In the drybox, Cp*(PMe₃)Ir(CH₃)₂ (46 mg, 0.113 mmol) and Cp*(PMe₃)IrCl₂ (80 mg, 0.170 mmol) were weighed into a Pyrex bomb. The apparatus was attached to a vacuum line, and dry, degassed CCl₄ (6 mL) was added by vacuum transfer. After being warmed to room temperature, the sealed vessel was heated to 80 °C in an oil bath for 36 h. The volatile materials were removed in vacuo, and the crude orange residue was purified by flash chromatography⁵⁴ on silica gel in the drybox. Elution with ether/hexane (50:50) afforded 80 mg (83%) of chloro methyl complex **5**. A second fraction, eluted with THF, contained the residual dichloro complex **5**. Analytical samples were obtained by recrystallization from hot hexanes or toluene layered with pentane and cooled to -40 °C: mp 139–141 °C; IR (KBr) 2804 (m), 2809 (m), 1210 (m) cm⁻¹, $\nu_{\text{Ir-CH}_3}$; ¹H NMR (C₆D₆) δ 1.47 (d, *J* = 1.9, C₅(CH₃)₅), 1.18 (d, *J* = 10.3, P(CH₃)₃), 1.08 (d, *J* = 7.0, Ir–CH₃); ¹³C{¹H} NMR (C₆D₆) δ 90.86 (d, *J* = 3.8, C₅Me₅), 13.88 (d, *J* = 37.2, P(CH₃)₃), 8.87 (s, C₅(CH₃)₅), -18.09 (d, *J* = 10.9, Ir–CH₃). Exact MS—three resolvable isotopomers for C₁₄H₂₇ClIrP: M⁺, calcd 456.1139, 454.1160, 452.1145, found 456.1148, 454.1133, 452.1123. Anal. Calcd for C₁₄H₂₇ClIrP: C, 37.04; H, 6.00. Found: C, 36.60; H, 6.16.

Cp*(PMe₃)Ir(CH₃)Cl (5) by Protonolysis^{1r,55} In the drybox, anilinium hydrochloride (127 mg, 0.976 mmol) was added in portions to a rapidly stirred solution of dimethyl complex **4** (423 mg, 0.976 mmol) in dry (MgSO₄) deoxygenated acetone (7 mL). Gas evolution began immediately, and the reaction mixture was stirred at room temperature for 1 h after all the solid had dissolved. The volatile materials were removed in vacuo and the orange residue was taken up in ether and filtered through silica gel. After dilution with an equal volume of hexane, the ether was removed slowly under reduced pressure, affording yellow crystals, 351 mg (79%), of >95% purity. An additional 89 mg (20%) of material of comparable purity was isolated upon evaporation of the mother liquors.

Cp*(PMe₃)Ir(CD₃)Cl (5-*d*₃). Protonolysis of Cp*(PMe₃)Ir(CD₃)₂ with anilinium hydrochloride proceeded as described above. No protium in the CD₃ ligand could be detected by ¹H NMR (<1% detection limit). IR (KBr) 2191 (m), 2108 (m), 2059 (m) cm⁻¹, $\nu_{\text{Ir-CD}_3}$; ¹H NMR (C₆D₆) δ 1.48 (d, *J* = 1.9, C₅(CH₃)₅), 1.19 (d, *J* = 10.2, P(CH₃)₃); ²H NMR (C₆H₆) δ 0.95 (d, *J* = 0.9, Ir–CD₃).

Cp*(PMe₃)Ir(CH₃)H (6)⁵³ In the drybox, chloromethyl complex **5** (145 mg, 0.320 mmol) was dissolved in THF (6 mL) and protected from room light.⁵⁶ An excess of lithium borohydride (>4 molar equiv) was added and the reaction mixture stirred at room temperature overnight. The volatile materials were removed slowly in vacuo and the residue was extracted with pentane and filtered through Celite. Removal of the pentane afforded the hydrido methyl complex **6**, which crystallized on standing. ¹H NMR integration showed this material (>95% yield) was contaminated with approximately 1% Cp*(PMe₃)IrH₂. An analytical sample was obtained by slow evaporation of pentane from a solution containing a few drops of hexamethyldisiloxane at -40 °C in the dark: IR (C₆D₆) 2090 cm⁻¹, $\nu_{\text{Ir-H}}$; ¹H NMR (C₆D₆) δ 1.87 (d, *J* = 1.5, C₅(CH₃)₅), 1.22 (d, *J* = 10.0, P(CH₃)₃), 0.70 (d, *J* = 6.0, Ir–CH₃), -17.23 (d, *J* = 37.9, Ir–H); ¹³C{¹H} NMR (C₆D₆) δ 91.15 (d, *J* = 3.9, C₅(CH₃)₅), 18.99 (d, *J* = 36.7, P(CH₃)₃), 10.11 (s, C₅(CH₃)₅), -37.96 (d, *J* = 8.9, Ir–CH₃).⁵⁷ Anal. Calcd for C₁₄H₂₈IrP: C, 40.08; H, 6.73. Found: C, 39.68; H, 6.46.

Cp*(PMe₃)Ir(CH₃)D (6-*d*₁). This was prepared as described above for **6**, except a large excess of sodium borodeuteride (98% atom *d*) and LiCl was used to form soluble LiBD₄ in situ. The extent of deuterium incorporation in the hydride position was 95% as measured by NMR integration using a long pulse delay. IR (C₆D₆) 1512 (s) cm⁻¹, $\nu_{\text{Ir-D}}$; ¹H NMR (C₆D₆) δ 1.87 (d, *J* = 1.5, C₅(CH₃)₅), 1.22 (d, *J* = 10.0, P(CH₃)₃),

(54) Still, W. C.; Kahn, M.; Miura, A. *J. Org. Chem.* 1978, 43, 2923. Rapid chromatography is necessary to prevent reequilibration of the chloromethyl complex. Material allowed to linger on the column elutes impure, containing a few percent of Cp*(PMe₃)Ir(Me)₂ and Cp*(PMe₃)Ir(Cl)₂.

(55) Anilinium hydrochloride was determined to be an effective source of HCl in this reaction by Dr. Jeffrey C. Hayes in these laboratories.

(56) In ambient light, the hydrido methyl complex **6** slowly decomposes to Cp*(PMe₃)IrH₂. The deuterium scrambling is also accelerated in the light.

(57) The ¹³C{¹H} NMR resonance for the iridium-bound methyl was misassigned in ref 53.

(53) Independently prepared by the reaction of [Cp*(PMe₃)Ir(H)]⁺Li⁻ with the alkyltrifluoromethyltoluene sulfonate. Gilbert, T. M.; Bergman, R. G. *J. Am. Chem. Soc.* 1985, 107, 3502–3507.

0.70 (d, $J = 6.0$, Ir-CH₃); ²H NMR (C₆H₆) δ -17.41 (d, $J = 5.5$, Ir-D).

Cp*(PMe₃)Ir(CD₃)D (6-d₄). This was prepared as above, except the deuterated chloro methyl complex, 5-d₃, was treated with NaBD₄/LiCl: IR (C₆D₆) 1500 (br) cm⁻¹, $\nu_{\text{Ir-D}}$; 2176, 2094, 2058 (m) cm⁻¹; ¹H NMR (C₆D₆) δ 1.87 (d, $J = 1.5$, C₃(CH₃)₃), 1.22 (d, $J = 10.0$, P(CH₃)₃); ²H NMR (C₆H₆) δ 0.59 (d, $J = 0.8$, Ir-CD₃), -17.11 (d, $J = 5.5$, Ir-D). The material contained 4% Cp*(PMe₃)Ir(CD₃)H by NMR integration at long pulse delay.

Thermolysis of Cp*(PMe₃)Ir(CH₃)D (6-d₁). In the drybox, 8 and 10 mg of 6-d₁ were loaded into each of two NMR tubes fused to ground glass joints. The tubes were protected from ambient light, attached to vacuum stopcocks and removed to a vacuum line. Degassed benzene-d₆ (0.7 mL) was added by vacuum transfer to both tubes, and to one was added trimethylphosphine (0.3 equiv by NMR integration). The tubes were sealed under vacuum and stored in the dark. No scrambling was observed after 24 h at room temperature in the dark. After the samples were heated at 125 °C for 18.5 h, ¹H NMR integration of both samples at long pulse delay indicated between 48 and 50% protium incorporation in the hydride position. After several days at 125 °C, the protium incorporation in the hydride position reached approximately 80%.

Thermolysis of Cp*(PMe₃)Ir(CH₃)H (6) with Cp*(PMe₃)Ir(CD₃)D (6-d₄). A degassed benzene-d₆ solution (1.0 mL) of methyl complexes 6 and 6-d₄ (16 mg, 0.04 M each) and trimethylphosphine (0.5 eq) was heated to 160 °C in a sealed NMR tube. After 9 h, ¹H NMR analysis indicated a 65% conversion of starting materials to Cp*(PMe₃)Ir(C₆D₅)D (2-d₆) and Cp*Ir(PMe₃)D₂ in a ratio of approximately 3.5:1. The solution was frozen at -196 °C, the NMR tube cracked open in a sealed apparatus,⁵⁸ and the head gases sampled directly by MS. Analysis revealed the presence of all possible labeled methanes CH_nD_{4-n} ($n = 0-4$) in significant amounts.

(58) The apparatus used will be described: Wenzel, T. T.; Bergman, R. G. *J. Am. Chem. Soc.*, in press.

Acknowledgment. This work was carried out under the auspices of a collaborative Lawrence Berkeley Laboratory/Industrial research project supported jointly by the Chevron Research Co., Richmond, CA, and the Director, Office of Energy Research, Office of Basic Energy Sciences, Chemical Sciences Division of the U.S. Department of Energy under Contract No. DE-AC03-76SF00098. J.M.S. acknowledges an NIH National Research Service Award (Grant No. F32-GM09289). Initial experiments to determine the equilibrium constant in the pentane-cyclohexane system were conducted by Dr. Caroline A. Kovac in these laboratories. The crystal structure analysis was performed by Dr. F. J. Hollander, staff crystallographer at the UC Berkeley X-ray crystallographic facility (CHEXRAY). Partial funding for the equipment in the facility was provided by the National Science Foundation through Grant No. CHE79-07027. The Bruker AM-500 NMR spectrometer was purchased with funds from NSF (No. CHE-8208994) and NIH (No. RR-02428) equipment grants. We are grateful to Mr. Rudi Nunlist for assistance in obtaining ¹H NMR spectra in hydrocarbon mixtures and to the Johnson-Matthey Co. for a loan of iridium trichloride. Tom Lawhead provided assistance in the design and fabrication of NMR sample tubes. The following individuals are thanked for the disclosure of results prior to publication: Profs. J. L. Beauchamp, R. H. Crabtree, J. Halpern, W. D. Jones, and J. R. Norton.

Supplementary Material Available: Crystal packing diagram for 1, molecular geometry and labeling scheme for molecule 2, hydrogen positional parameters and their estimated standard deviations, and listings of F_o and F_c (52 pages). Ordering information is given on any current masthead page.

Synthetic, Structural, and Theoretical Studies of η^2 -Acyl Complexes of Molybdenum

M. David Curtis,* Kom-Bei Shiu, and William M. Butler

Contribution from the Department of Chemistry, The University of Michigan, Ann Arbor, Michigan 48109. Received June 24, 1985

Abstract: Hydridotrakis(pyrazolyl)borate (Tp) complexes of the type TpMo(CO)₂(η^2 -COR) (R = Me (1), Ph (2)) are formed from the reaction of TpMo(CO)₃⁻ with MeI, Me₃O⁺, MeCOBr, or PhCOBr. The use of ¹³C-labeled PhC*OBr in the reaction established that a carbonyl initially on the metal is lost in the decarbonylation and that the η^2 -acyl is not in equilibrium with a low concentration of the isomeric σ -alkyltricarbonyl complex. The derivatives Tp(CO)LMo(η^2 -COMe) (L = P(OMe)₃ (3) and PEt₃ (4)) are made from 1 and the appropriate phosphine. The structures of 1-4 were determined by X-ray crystallography: (1) a , b , and $c = 8.995$ (3), 12.803 (4), and 14.999 (6) Å; $\beta = 103.98$ (3)°; $V = 1677$ (1) Å³; $Z = 4$; space group $P2_1/n$ (no. 14); (2) a , b , and $c = 9.405$ (2), 12.505 (3), and 9.025 (2) Å; α , β , and $\gamma = 114.59$ (2), 92.85 (2), and 95.45 (2)°; $V = 956.0$ (4) Å³; $Z = 2$; space group = $P\bar{1}$ (no. 2); (3) a , b , and $c = 8.953$ (2), 15.684 (6), and 8.032 (4) Å; α , β , and $\gamma = 99.47$ (4), 102.79 (3), and 97.78 (3)°; $V = 1067.5$ (7) Å³; $Z = 2$; space group = $P\bar{1}$. Values of R_1 and R_2 for 1-4 are 0.045, 0.059 (1); 0.038, 0.063 (2); 0.038, 0.056 (3); and 0.044, 0.061 (4). The bonding of an L₅M (d⁴) fragment to the η^2 -acyl group, the rotational conformations of the latter, and the relative stabilities of Cp(CO)₂Mo(η^2 -HCO), Cp(CO)₃Mo-H, (N-donor)₃(CO)₂Mo(η^2 -HCO), and (N-donor)₃(CO)₃Mo-H are comprehensively treated within the framework of the Extended Hückel MO formalism. It is shown that there is substantial double-bond character in the Mo=C(acyl) bond but a very weak Mo-O bond and that the compounds should be regarded as stabilized 16-electron complexes. There is an inherent tendency toward a bending distortion in the L₅M fragment, and the η^2 -acyl group tends to be aligned with the axis of distortion and/or with the M-CO bond(s).

The preparation of η^2 -acyl complexes and their chemical properties have been the subject of much recent research.¹⁻¹¹ This

interest is derived in part from the possible role of η^2 -acyl and η^2 -formyl structures in metal-catalyzed hydrogenation of carbon

(1) (a) Fachinetti, G.; Fochi, G.; Floriani, C. *J. Chem. Soc. Dalton Trans.* 1977, 1946. (b) Fachinetti, G.; Floriani, C.; Stockli-Evans, H. *Ibid.* 1977, 2297. (c) Fachinetti, G.; Floriani, C.; Marchetti, F.; Medino, S. *J. Chem. Soc., Chem. Commun.* 1976, 522.

(2) (a) Erker, G.; Rosenfeldt, F. *Angew. Chem., Int. Ed. Engl.* 1978, 17, 605. (b) *J. Organomet. Chem.* 1980, 188, C1.

(3) Strauss, O. A.; Grubbs, R. H. *J. Am. Chem. Soc.* 1982, 104, 5499.

(4) Marsella, J. A.; Caulton, K. G. *J. Am. Chem. Soc.* 1980, 102, 1747.